Article

Not peer-reviewed version

Effect of the Temperature on the Polar and Lewis Acid-Base properties of the Adsorption of PMMA on Silica by Inverse Gas Chromatography

Tayssir Hamieh *

Posted Date: 18 March 2024

doi: 10.20944/preprints202403.0997.v1

Keywords: London dispersion equation; recovery fraction; polar enthalpy and entropy; Lewis's acid-base parameters, transition temperatures; intermolecular separation distance

Article

Effect of the Temperature on the Polar and Lewis Acid-Base Properties of the Adsorption of PMMA on Silica by Inverse Gas Chromatography

Tayssir Hamieh [1,2]

[1] Faculty of Science and Engineering, Maastricht University, P.O. Box 616, 6200 MD Maastricht, The Netherlands; t.hamieh@maastrichtuniversity.nl

[2] Laboratory of Materials, Catalysis, Environment and Analytical Methods Laboratory (MCEMA), Faculty of Sciences, Lebanese University, Hadath, Beirut, P.O. Box 6573/14 Badaro, Lebanon

Abstract: The temperature effect plays an important role for an accurate determination of the polar free energy, polar thermodynamic parameters, and enthalpic and entropic Lewis's acid base properties of oxides, polymers and composites polymers/oxides. The adsorption of polymers on other solid surfaces is crucial in many industrial applications, coatings, paints, catalysis, colloids and adhesion processes. (1) Background: Inverse gas chromatography at infinite was used for the physicochemical characterization of solid substrates by determining the thermodynamic parameters of adsorption of model organic solvents on solid surfaces such as polymers, metallic oxides, carbon fibers, pharmaceutical or 3D/4D printing substrates. (2) Methods: A new method based on the London dispersion equation was applied with a new parameter associating the deformation polarizability and the harmonic mean of the ionization energies of solvent. More accurate values of the dispersive and polar interaction energies of the various organic solvents adsorbed on PMMA in bulk phase and PMMA/silica at different recovery fractions were obtained as well as the Lewis acid-base parameters and the transition temperatures of the different composites. (3) Results: This new methodology gave very interesting results on the behavior of PMMA adsorbed on silica. An important effect of the temperature and the recovery fraction on the various physicochemical and thermodynamic properties was highlighted. The variations of all interaction parameters showed the presence of three transition temperatures for the different PMMA adsorbed on silica with the various coverage rates with a shift of these temperatures for a recovery fraction of 31% (4) Conclusions: An important variation of the polar enthalpy and entropy of adsorption, the Lewis acid-base parameters and the intermolecular separation distance as a function of the temperature and the recovery fraction of PMMA on silica.

Keywords: London dispersion equation; recovery fraction; polar enthalpy and entropy; Lewis's acid-base parameters; transition temperatures; intermolecular separation distance

1. Introduction

The determination of physicochemical properties of polymers adsorbed on oxides play an important role in various industrial applications and chemical processes, including **specific composites** such as plastics, paper, and rubber [1]. The surface modification of polymers by adsorption on metallic oxides is crucial in several industrial processes and products [1–10]. Indeed, the adsorption of polymer on solid surfaces, in a solvent, is very useful for the dispersion or aggregation of concentrated suspensions or slurries. The adsorption process can contribute to the strength of the polymer segment contacts in the areas of adhesives, coatings and polymer composites. For example, the physicochemical and mechanical properties of polymer composites are not only affected by the adhesion strength between polymer and reinforced filler but also by the variations of the temperature.

The behavior of polymer composites strongly depends on the values of the transition temperatures and more particularly on their glass transitions. Polymers have different types of behavior, around the glass temperature (T_g) depending on the temperature in the glass and liquid

 doi:10.20944/preprints202403.0997.v1

states. Most physical properties, including, for example, the enthalpy, rheological, and other surface properties change with temperature and time until reaching equilibrium, if polymers are heated below T_g [8–12]. This is directly related to the physical aging or structure relaxation of polymers or devices made of glassy polymers [13,14].

The determination of the physicochemical properties of polymers adsorbed on oxides is required to prevent their behaviors in the contact with other solids, liquids or gas. The composites polymer/metallic oxides are very used for the coatings of paintings or industrial packing. Polymer composites or nanocomposites, such as acrylate polymers or poly methyl methacrylate (PMMA) adsorbed on oxides can be used in many applications such as, artificial muscles, urban furniture, aeronautics, and microelectronics due to their high mechanical properties and high capacitance density [8,15–21].

Many studies were interested in the determination of the physicochemical properties [22–46] and the glass transition temperatures [47–58] by inverse gas chromatography (IGC) at infinite dilution. This technique was applied to quantify the interactions between polymers, composites or oxides and organic molecules under the of infinite dilution conditions [22–58]. The Lewis acid–base properties of insulating thermoplastic and thermosetting polymer materials [13,14,47–58], and the solubility parameters in appropriate solvents were also determined by IGC technique. Papirer et al. [59] have studied the effect of surface acid–base characteristics of PMMA adsorbed on alumina, whereas, Hamieh et al. [55–58] have highlighted the presence of three transition temperatures of PMMA in the bulk phase and when adsorbed on silica and alumina.

However, the effect of the temperature change on the polar interactions and the Lewis acid-base properties near the transition temperatures of PMMA adsorbed on silica has never yet studied in literature.

We proposed in this paper to use IGC technique at infinite dilution to study the impact of the variation of the temperature on the London dispersive and polar free interaction energy, and Lewis's acid-base parameters of PMMA/silica system for different recovery fractions of PMMA adsorbed on silica by applying our new methodology. Indeed, this recent method used the London dispersion equation [44,45] and proposed a new thermodynamic parameter $\mathcal{P}_{SX}$ using the deformation polarizability α_{0X} of the probe and the ionization energies of the solid ε_S and the solvent ε_X following this relation:

$$\mathcal{P}_{SX} = \frac{\varepsilon_S\, \varepsilon_X}{(\varepsilon_S + \varepsilon_X)} \alpha_{0X} \qquad (1)$$

By using the parameter $\mathcal{P}_{SX}$, it was possible to obtain accurate values of the free interaction energy between the solid surfaces and the adsorbed organic molecules. The separation between the dispersive and polar interaction energies of PMMA adsorbed on silica at various recovery fractions allowed us to obtain the polar enthalpy and entropy of adsorption and the surface acid-base parameters of the composite PMMA/silica, such as the enthalpic and entropic Lewis's acid-base constants of the solid substrates.

2. Chromatographic Methods and Materials

The net retention time t_n and volume V_n of n-alkanes and polar molecules adsorbed on PMMA/silica surfaces were experimentally obtained by using the inverse gas chromatography (IGC) at infinite dilution [22–59]. This led to the free energy of adsorption ΔG_a^0 of adsorbed solvents on the solid surface (Equation 1):

$$\Delta G_a^0 = -RT\, lnV_n + B(T) \qquad (1)$$

Where T is the absolute temperature of the chromatographic column containing the solid material, R the perfect gas constant, and $B(T)$ a constant depending on the temperature and reference characteristics referred to the two-dimensional state of adsorbed film.

ΔG_a^0 is equal to the sum of the London dispersion component ΔG_a^d and the polar component ΔG_a^p of the free energy adsorption (Equation 2)

$$\Delta G_a^0 = \Delta G_a^d + \Delta G_a^p \qquad (2)$$

 doi:10.20944/preprints202403.0997.v1

The London dispersion free energy can be expressed as:

$$\Delta G_a^d(T) = -\frac{\alpha_{0S}}{H^6}\left[\frac{3\mathcal{N}}{2(4\pi\varepsilon_0)^2}\left(\frac{\varepsilon_S\,\varepsilon_X}{(\varepsilon_S+\varepsilon_X)}\alpha_{0X}\right)\right] \quad (3)$$

Where and $\mathcal{N}$ is the Avogadro's number, ε_0 the permittivity of vacuum, S denoting the solid particle and X the solvent molecule separated by a distance H, and ε_S and ε_X are the respective ionization energies of the solid and the solvent ε_X. The new chromatographic chosen parameter of interaction between the solid and the solvent is given by

$$\mathcal{P}_{SX} = \frac{\varepsilon_S\,\varepsilon_X}{(\varepsilon_S+\varepsilon_X)}\alpha_{0X} \quad (4)$$

In the case of n-alkanes (C_n) adsorbed on the solid material, $RTlnVn(C_n)$ can be given by:

$$RTlnVn(C_n) = A\left[\frac{3\mathcal{N}}{2(4\pi\varepsilon_0)^2}\mathcal{P}_{SX}(C_n)\right] - B \quad (5)$$

Where A is given by:

$$A = \frac{\alpha_{0S}}{H^6} \quad (6)$$

The straight-line of n-alkanes representing the variations of $RTlnVn(C_n)$ against $\frac{3\mathcal{N}}{2(4\pi\varepsilon_0)^2}\mathcal{P}_{SX}(C_n)$ allowed us to determine the polar free energy $\left(-\Delta G_a^p(T)\right)$ of polar solvents adsorbed on PMMA/silica composites as a function of the temperature by using the following equation:

$$-\Delta G_a^p(T) = RTlnVn(X) - A\left[\frac{3\mathcal{N}}{2(4\pi\varepsilon_0)^2}\mathcal{P}_{S-X}\right] + B \quad (7)$$

The polar enthalpy $-\Delta H_a^p(T)$ and entropy $-\Delta S_a^p(T)$ of organic molecules were then determined from the variations of $\left(-\Delta G_a^p(T)\right)$ using the following thermodynamic relations:

$$\Delta H_a^p(T) = \frac{\partial\left(\frac{\Delta G_a^p(T)}{T}\right)}{\partial\left(\frac{1}{T}\right)} \quad (8)$$

$$\Delta S_a^p(T) = -\left(\frac{\partial\left(\Delta G_a^p(T)\right)}{\partial T}\right) \quad (9)$$

The values of $-\Delta H_a^p(T)$ and $-\Delta S_a^p(T)$ of adsorbed polar solvents were obtained as a function of the temperature and allowed us to quantify the Lewis's enthalpic acid base constants $K_A(T)$ and $K_D(T)$, and entropic acid base parameters $\omega_A(T)$ and $\omega_D(T)$ with respect of the temperature:

$$-\Delta H^p(T) = DN \times K_A(T) + AN \times K_D(T) \quad (10)$$

$$-\Delta S^p(T) = DN \times \omega_A(T) + AN \times \omega_D(T) \quad (11)$$

Where *AN* and *DN* are respectively the Gutmann electron donor and acceptor numbers of the polar solvents [60]. The used values were those corrected by Riddle and Fowkes [61].

The model organic molecules used as probes to quantify their interactions with the composites PMMA/silica were the following:

- the n-alkanes such as n-pentane, n-hexane, n-heptane, n-octane, and n-nonane
- the polar molecules, divided into three groups:
  - Lewis's acid solvents such as dichloromethane, chloroform, and carbon tetrachloride
  - Basic solvent such as ethyl acetate, diethyl ether, tetrahydrofuran
  - Amphoteric such as toluene

PMMA and silica solid particles with different recovery fractions of adsorbed polymer used in this work were the same solid materials previously characterized in other studies by using other models and chromatographic methods [39,55,62]. The previous experimental data of $RTlnVn$ of the various probes adsorbed on PMMA/silica composites obtained from IGC technique at infinite dilution was used to study the effect of the temperature on the various thermodynamic and physicochemical parameters of the adsorption of PMMA on silica at different recovery fractions.

3. Experimental Results

 doi:10.20944/preprints202403.0997.v1

3.1. Polar Surface Interactions between PMMA/Silica and Solvents

The Handbook of Physics and Chemistry [63] allowed giving on Table S1 to S3 (in Supplementary Materials) the respective values of deformation polarizability α_{0X} and parameter $\frac{3\mathcal{N}}{2(4\pi\varepsilon_0)^2}\mathcal{P}_{S-X}$ of the various molecules adsorbed on PMMA and silica. Using the values given in Tables S1–S3, the polar free surface energy ($-\Delta G_a^p(T)$) of the polar probes adsorbed on the different solid composites were determined. Tables 1–5 gave the obtained of ($-\Delta G_a^p(T)$) relative to PMMA adsorbed on silica by varying the recovery fraction.

Table 1. Values of ($-\Delta G_a^p(T)$ kJ/mol) of polar molecules adsorbed on silica particles as a function of the temperature.

Polar free energy of Solvents adsorbed on silica							
Temperature T(K)	CCl_4	CH_2Cl_2	$CHCl_3$	Diethyl ether	THF	Ethyl acetate	Toluene
303.15	6.674	25.241	20.030	28.337	37.697	17.422	17.701
313.15	6.715	24.896	19.854	27.581	36.486	17.089	17.452
323.15	6.752	24.807	19.752	26.838	35.506	16.852	17.328
328.15	6.777	24.379	19.590	26.447	34.669	16.590	17.078
333.15	6.797	24.206	19.502	26.069	34.064	16.423	16.954
338.15	6.818	24.034	19.414	25.691	33.458	16.257	16.829
343.15	6.809	23.876	19.303	25.462	32.786	16.149	16.722
348.15	6.859	23.689	19.238	24.935	32.247	15.924	16.580
353.15	6.879	23.516	19.150	24.557	31.642	15.757	16.456
363.15	6.884	23.102	18.927	23.805	30.437	15.394	16.170
373.15	6.961	22.826	18.798	23.045	29.220	15.091	15.958
378.15	6.982	22.654	18.710	22.667	28.614	14.925	15.833
383.15	6.969	22.285	18.547	22.315	27.908	14.704	15.598
388.15	7.023	22.309	18.534	21.911	27.403	14.592	15.584
393.15	7.043	22.136	18.446	21.533	26.798	14.425	15.460
398.15	7.064	21.964	18.358	21.155	26.192	14.259	15.335
403.15	7.127	21.689	18.248	20.674	25.592	14.080	15.184
408.15	7.105	21.619	18.182	20.399	24.981	13.926	15.086
413.15	7.125	21.446	18.094	20.021	24.376	13.759	14.962
423.15	7.205	21.206	18.006	19.185	23.401	13.498	14.834
433.15	7.207	20.756	17.742	18.509	21.954	13.093	14.464
443.15	7.248	20.411	17.566	17.753	20.743	12.760	14.215
453.15	7.289	20.066	17.390	16.997	19.532	12.427	13.966
463.15	7.348	20.070	17.346	16.496	18.659	12.350	13.973
473.15	7.371	19.376	17.038	15.485	17.110	11.761	13.468

Table 2. Values of ($-\Delta G_a^p(T)$ kJ/mol) of polar molecules adsorbed on PMMA particles as a function of the temperature.

Polar free energy of Solvents adsorbed on PMMA							
Temperature T(K)	CCl_4	CH_2Cl_2	$CHCl_3$	Diethyl ether	THF	Ethyl acetate	Toluene
303.15	10.765	18.520	16.079	15.039	19.851	16.029	13.204

 doi:10.20944/preprints202403.0997.v1

313.15	10.254	16.940	14.930	13.956	18.940	14.694	12.212
323.15	10.294	16.034	15.101	14.437	18.822	14.037	11.443
328.15	10.808	15.902	15.552	15.362	19.155	14.498	11.677
333.15	11.434	17.105	16.068	16.544	19.846	15.192	12.190
338.15	9.631	14.792	13.161	13.037	17.712	13.243	10.501
343.15	10.629	15.055	14.098	13.685	18.247	13.912	11.245
348.15	11.414	15.178	15.013	14.115	18.667	14.430	11.989
353.15	11.721	14.911	14.782	13.980	18.464	14.285	11.936
363.15	10.816	13.717	12.961	12.873	17.352	13.499	10.680
373.15	10.821	12.279	9.454	11.020	16.585	12.891	10.111
378.15	11.206	13.019	10.825	10.962	17.252	13.325	10.604
383.15	11.772	14.521	12.968	12.321	18.652	14.659	12.181
388.15	12.487	10.832	12.193	10.936	16.403	11.700	9.624
393.15	10.950	12.707	11.533	11.870	15.718	10.781	8.900
398.15	11.029	12.170	10.930	11.397	15.638	12.783	10.237
403.15	11.465	11.776	10.791	11.399	15.942	13.202	10.136
408.15	11.830	11.631	10.794	11.360	16.258	13.460	10.355
413.15	11.758	11.135	10.040	10.942	16.106	13.146	10.197
423.15	11.929	11.458	10.113	11.090	17.047	13.434	10.433
433.15	13.579	13.574	11.582	12.569	19.030	15.576	12.048
443.15	12.136	10.220	8.929	9.901	15.065	13.114	10.016
453.15	12.047	9.388	7.939	9.244	14.165	12.620	9.682
463.15	12.299	8.917	7.617	9.151	13.848	12.645	9.287
473.15	11.924	7.776	6.642	8.470	12.938	11.811	8.280

Table 3. Values of $(-\Delta G_a^p(T)$ kJ/mol) of polar molecules adsorbed on the system PMMA/silica as a function of the temperature for a recovery fraction $\theta = 0.31$.

Polar free energy of Solvents adsorbed on PMMA/silica for $\theta = 0.31$							
Temperature T(K)	CCl_4	CH_2Cl_2	$CHCl_3$	Diethyl ether	THF	Ethyl acetate	Toluene
303.15	6.698	20.777	15.865	16.603	20.647	14.300	14.620
313.15	6.055	19.604	14.885	15.493	18.449	12.803	13.694
323.15	5.932	18.973	14.390	14.799	17.228	12.216	13.726
328.15	5.704	18.169	13.853	14.282	16.141	11.486	13.530
333.15	6.253	18.442	14.047	14.603	16.362	11.672	14.064
338.15	6.519	18.608	14.218	13.973	16.216	11.637	14.235
343.15	6.605	19.382	14.562	13.340	15.835	11.926	14.005
348.15	6.730	18.336	12.890	12.001	14.743	10.618	13.470
353.15	7.264	18.364	13.507	12.453	14.008	10.503	13.290
363.15	6.952	18.115	13.879	11.315	12.626	9.424	13.254
373.15	6.584	17.019	12.869	9.437	10.630	7.416	12.282
378.15	6.844	17.200	13.082	8.936	10.315	7.107	12.492
383.15	6.714	16.865	12.933	8.706	9.823	6.584	12.327

 doi:10.20944/preprints202403.0997.v1

388.15	7.111	17.412	13.320	9.047	10.139	6.829	12.940
393.15	7.605	18.243	13.964	9.984	10.797	7.413	13.547
398.15	8.913	19.648	15.146	11.268	12.232	8.909	14.775
403.15	11.229	21.423	17.010	11.072	12.576	8.802	16.772
408.15	10.654	19.980	15.734	11.281	11.759	7.117	15.461
413.15	9.879	18.756	14.746	8.496	9.743	7.482	12.252
423.15	8.281	17.133	13.433	6.152	6.444	7.003	12.634
433.15	8.092	16.598	13.170	6.621	7.368	7.619	13.247
443.15	12.550	21.255	17.518	8.654	8.665	11.397	16.279
453.15	10.367	18.117	14.996	10.447	8.862	11.040	14.673
463.15	8.354	15.912	12.490	10.442	1.559	9.852	11.573
473.15	7.697	12.895	10.572	9.325	0.595	8.197	8.969

Table 4. Values of $(-\Delta G_a^p(T)$ kJ/mol) of polar molecules adsorbed on the system PMMA/silica as a function of the temperature for a recovery fraction $\theta = 0.83$.

Polar free energy of Solvents adsorbed on PMMA/silica for $\theta = 0.83$							
Temperature T(K)	CCl_4	CH_2Cl_2	$CHCl_3$	Diethyl ether	THF	Ethyl acetate	Toluene
303.15	7.773	27.605	23.019	21.816	25.479	20.114	17.258
313.15	7.219	25.780	21.588	20.382	24.106	18.354	15.812
323.15	7.726	24.330	20.823	19.402	23.091	16.800	15.052
328.15	7.983	24.125	20.151	19.158	22.906	16.021	14.985
333.15	8.322	24.143	20.132	18.742	22.962	15.604	15.539
338.15	8.421	24.970	20.394	18.368	23.217	16.923	15.672
343.15	7.970	23.919	20.547	18.073	21.957	16.634	14.982
348.15	8.213	23.804	20.465	17.719	21.787	16.379	15.316
353.15	8.480	23.752	20.339	17.763	21.690	16.315	15.442
363.15	7.946	22.566	19.802	16.558	19.764	14.651	13.973
373.15	7.400	21.338	18.643	15.259	18.336	12.867	13.259
378.15	7.177	21.114	18.505	14.790	17.504	12.511	12.966
383.15	8.088	21.872	19.412	15.216	18.162	13.086	13.592
388.15	9.738	23.872	20.633	17.249	20.357	14.790	15.021
393.15	7.975	22.237	18.677	16.071	19.312	12.425	13.092
398.15	7.579	21.453	18.849	14.284	17.365	9.449	10.478
403.15	8.266	21.428	19.153	13.895	17.001	11.597	13.409
408.15	8.378	20.973	18.729	13.601	16.463	11.654	13.423
413.15	8.176	20.481	18.274	13.057	15.661	11.281	13.111
423.15	8.263	20.132	18.597	12.392	14.863	11.137	12.497
433.15	9.011	21.753	19.964	13.615	16.245	12.413	13.101
443.15	8.413	19.670	18.315	11.083	13.556	10.859	12.321
453.15	8.373	19.017	17.896	10.411	12.693	10.113	12.024
463.15	11.973	22.320	21.465	13.227	15.364	12.954	15.267
473.15	8.067	17.745	16.842	8.413	10.414	7.945	10.717

 doi:10.20944/preprints202403.0997.v1

Table 5. Values of $(-\Delta G_a^p(T)$ kJ/mol) of polar molecules adsorbed on the system PMMA/silica as a function of the temperature for a recovery fraction $\theta = 1$.

Polar free energy of Solvents adsorbed on PMMA/silica for $\theta = 1$							
Temperature T(K)	CCl_4	CH_2Cl_2	$CHCl_3$	Diethyl ether	THF	Ethyl acetate	Toluene
303.15	13.797	36.031	32.260	30.623	38.590	21.479	26.098
313.15	13.567	31.827	28.141	27.132	33.996	20.360	23.011
323.15	12.594	27.832	24.874	23.581	28.575	18.376	20.293
328.15	12.366	26.052	22.043	21.509	26.236	17.682	17.852
333.15	12.572	25.107	21.512	20.173	24.834	17.746	17.145
338.15	11.175	23.004	19.957	18.075	22.883	17.019	15.721
343.15	7.827	22.303	19.418	17.043	22.426	16.908	15.316
348.15	8.731	23.918	21.243	17.929	23.166	17.644	16.472
353.15	9.682	24.387	21.614	18.557	23.527	17.500	17.214
363.15	11.294	24.438	22.228	19.161	23.921	16.971	17.656
373.15	11.607	23.218	21.724	18.422	22.395	15.990	16.949
378.15	11.599	23.350	21.692	18.202	22.230	16.213	17.043
383.15	12.922	25.912	23.757	19.957	24.657	18.321	18.608
388.15	14.514	28.129	25.061	21.098	23.208	20.016	17.299
393.15	11.630	25.838	23.488	18.299	21.089	17.162	14.154
398.15	9.405	22.887	20.451	15.594	19.094	15.325	12.647
403.15	7.366	18.964	17.081	12.048	17.162	14.041	13.030
408.15	7.781	18.878	17.221	12.010	16.629	13.365	13.403
413.15	8.249	19.192	17.691	12.004	16.478	13.009	13.687
423.15	9.622	19.875	18.807	12.975	17.161	13.139	14.195
433.15	8.548	17.697	16.005	9.842	15.043	14.366	12.628
443.15	5.562	14.849	14.031	7.101	11.750	12.211	9.983
453.15	6.883	15.433	14.892	7.366	11.880	12.355	11.138
463.15	8.179	16.389	16.175	8.339	12.549	12.883	11.825
473.15	8.812	16.525	16.477	8.298	12.238	12.504	11.793

The results in Table 1 showed that the silica particles presented higher polar interaction free energy with the base solvents and lower interaction energy with the acidic solvents. This led to conclude that silica particle surfaces exhibited stronger acidity than the other solid materials (PMMA/silica) and lower basic character. On the contrary, the values in Table 2 relative to PMMA particles showed higher basic character and lower acid interaction energy. With a recovery fraction of 31% of PMMA adsorbed on silica, it was observed that the acidic character of silica decreases while its basicity increases to reach a maximum for 100% of recovery fraction (for one monolayer). The effects of the temperature and the recovery fraction of PMMA adsorbed on silica were shown on Figures 1–7 for the various polar solvents used in this study.

Preprints.org (www.preprints.org) | NOT PEER-REVIEWED | Posted: 18 March 2024 doi:10.20944/preprints202403.0997.v1

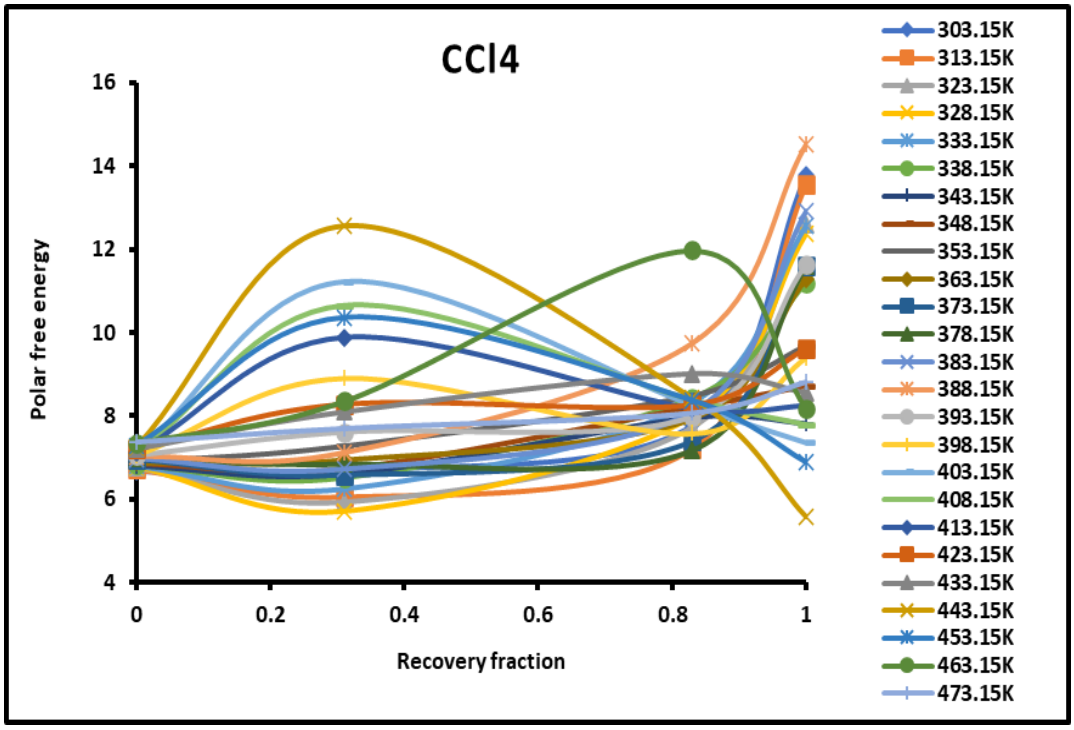

Figure 1. Evolution of the polar free interaction energy $(-\Delta G_a^p(T)$ (kJ/mol) of CCl_4 as a function of the recovery fraction of PMMA adsorbed on silica at different temperatures.

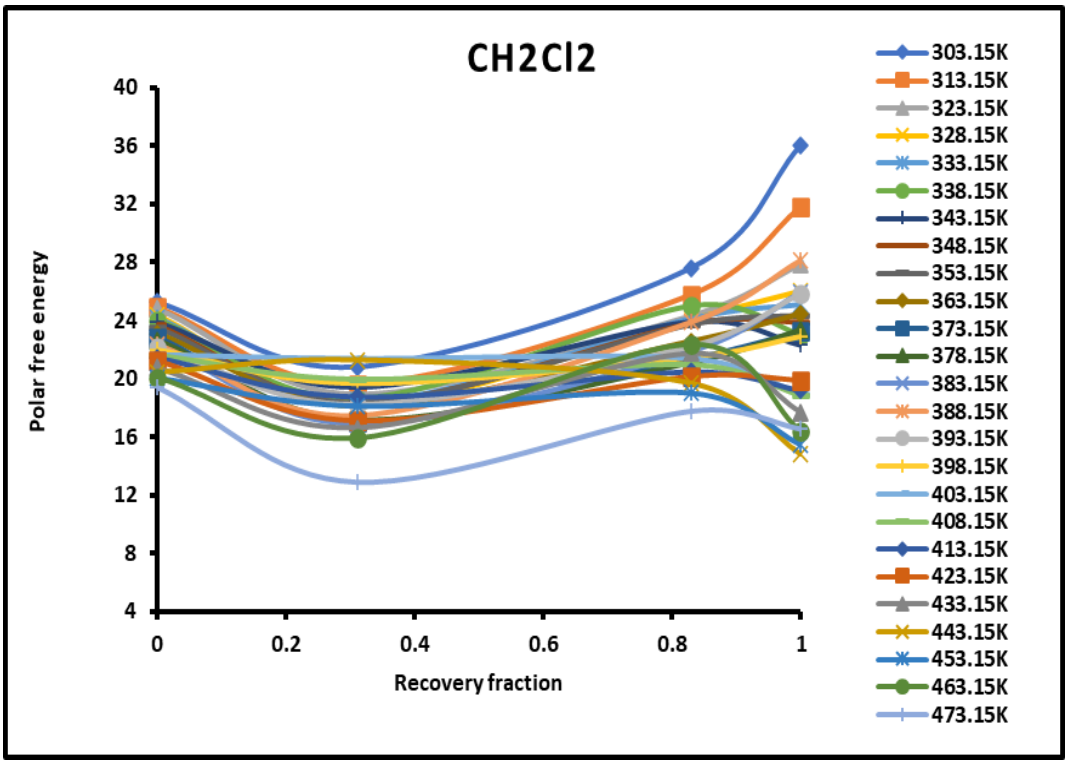

Figure 2. Evolution of the polar free interaction energy $(-\Delta G_a^p(T)$ (kJ/mol) of CH_2Cl_2 as a function of the recovery fraction of PMMA adsorbed on silica at different temperatures.

Preprints.org (www.preprints.org) | NOT PEER-REVIEWED | Posted: 18 March 2024 doi:10.20944/preprints202403.0997.v1

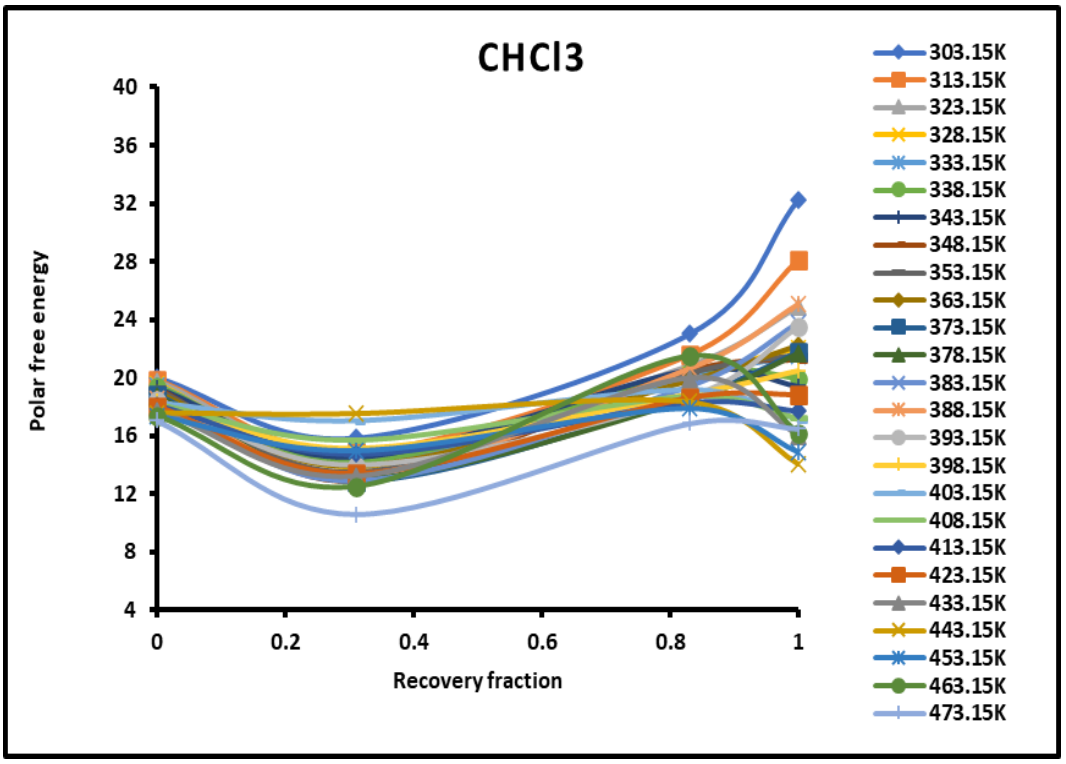

Figure 3. Evolution of the polar free interaction energy $(-\Delta G_a^p(T)$ (kJ/mol) of $CHCl_3$ as a function of the recovery fraction of PMMA adsorbed on silica at different temperatures.

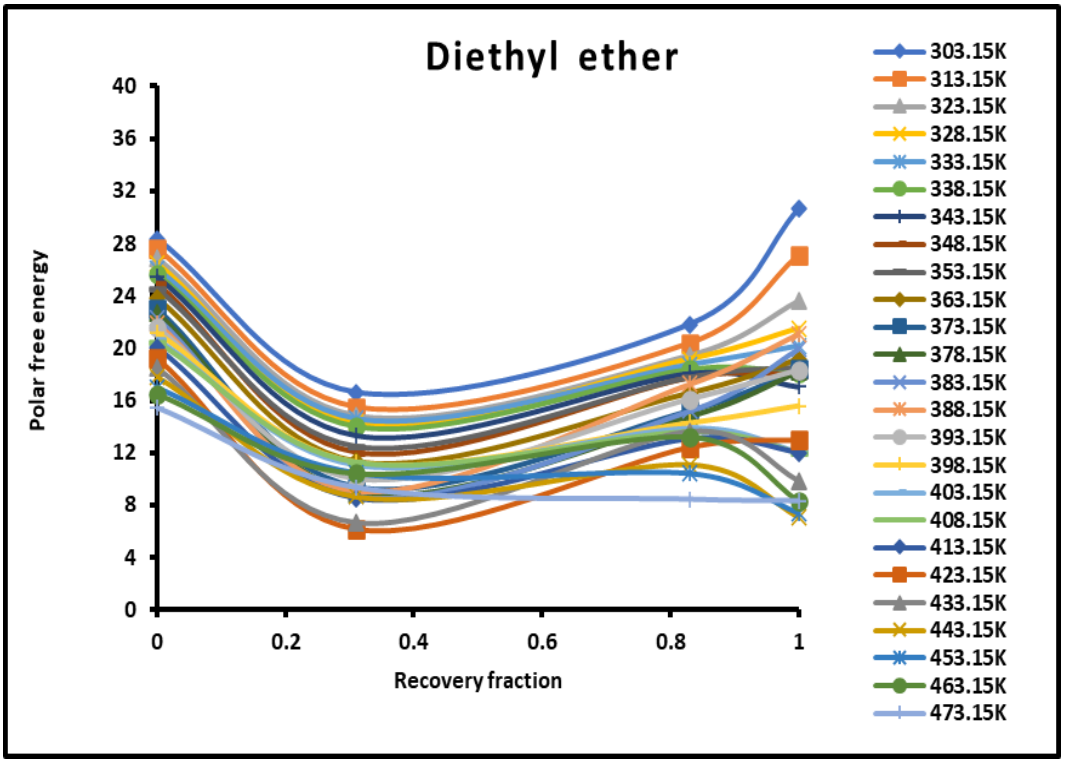

Figure 4. Evolution of the polar free interaction energy $(-\Delta G_a^p(T)$ (kJ/mol) of diethyl ether as a function of the recovery fraction of PMMA adsorbed on silica at different temperatures.

Preprints.org (www.preprints.org) | NOT PEER-REVIEWED | Posted: 18 March 2024 doi:10.20944/preprints202403.0997.v1

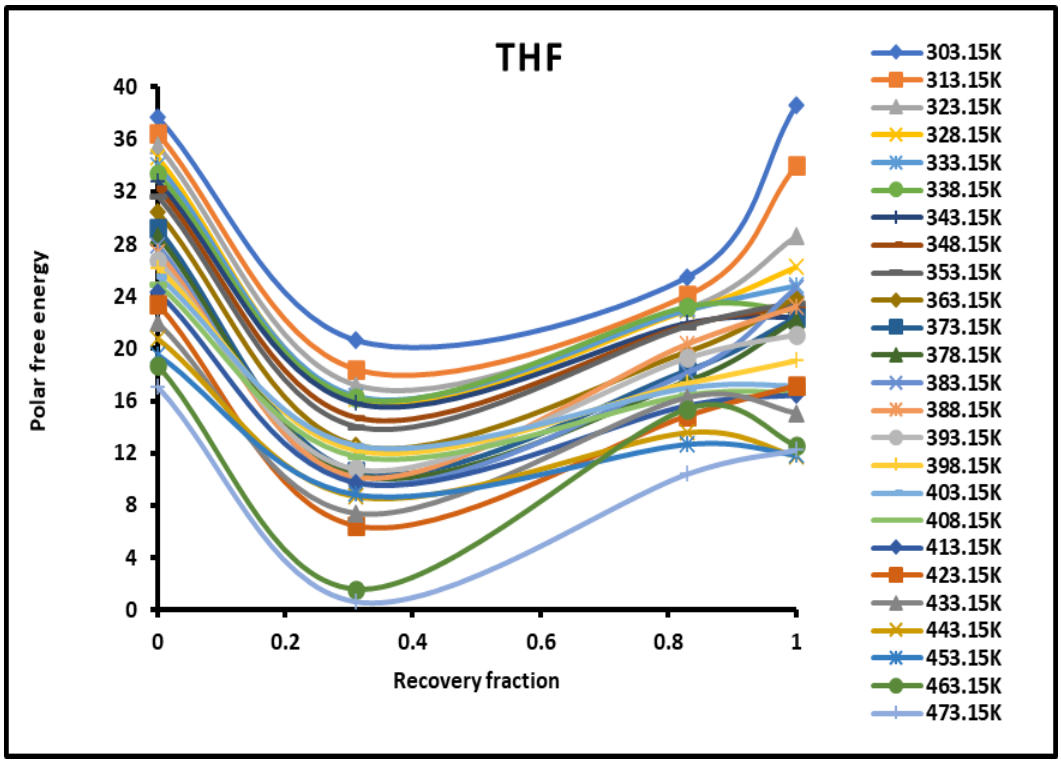

Figure 5. Evolution of the polar free interaction energy $(-\Delta G_a^p(T)$ (kJ/mol) of tetrahydrofuran (THF) as a function of the recovery fraction of PMMA adsorbed on silica at different temperatures.

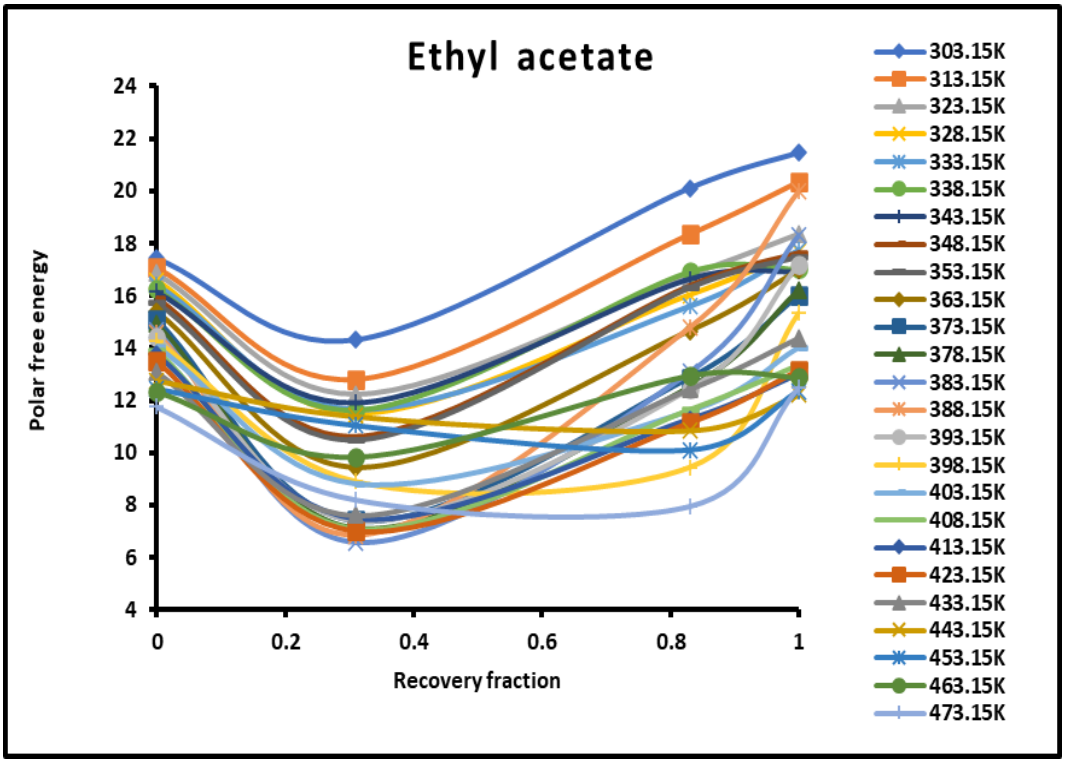

Figure 6. Evolution of the polar free interaction energy $(-\Delta G_a^p(T)$ (kJ/mol) of ethyl acetate as a function of the recovery fraction of PMMA adsorbed on silica at different temperatures.

 doi:10.20944/preprints202403.0997.v1

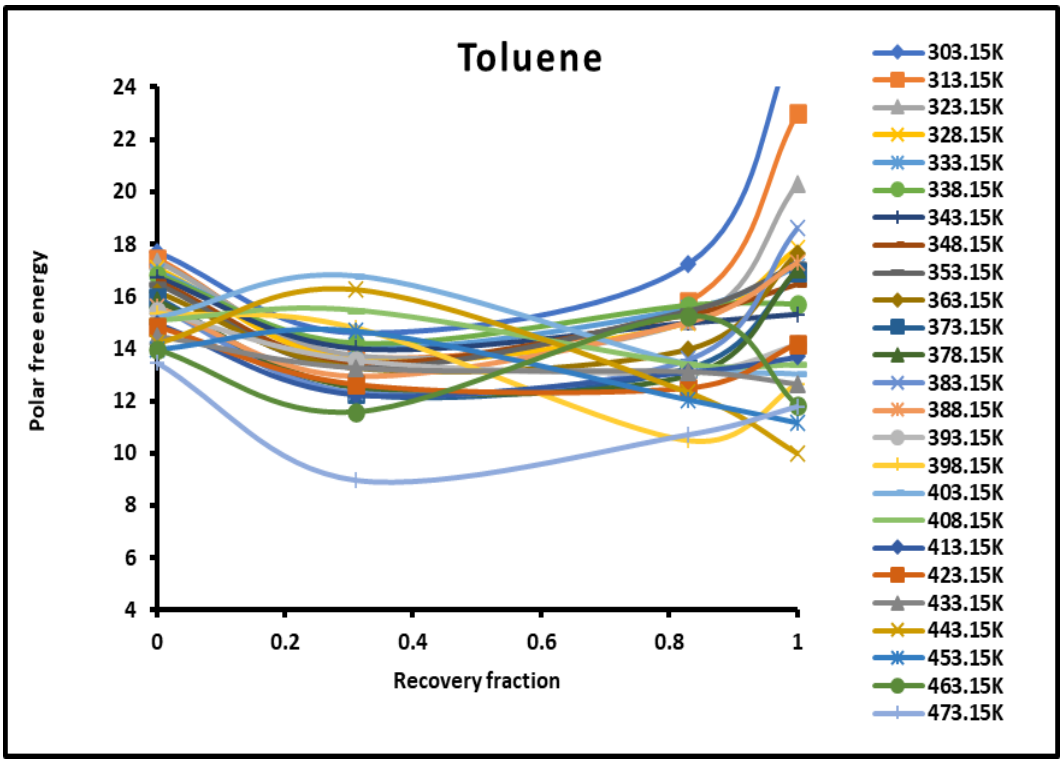

Figure 7. Evolution of the polar free interaction energy $(-\Delta G_a^p(T)$ (kJ/mol) of toluene as a function of the recovery fraction of PMMA adsorbed on silica at different temperatures.

The study of the evolution of the polar free interaction energy of the various polar solvents adsorbed on the composites PMMA/silica with respect of the recovery fraction and temperature (Figure 1–7) showed a certain decrease of $(-\Delta G_a^p(T)$ until a recovery fraction of 31% followed by an increase of the polar free interaction energy to reach a maximum when the coverage rate reaches 100% (case of monolayer) at all temperatures excepted for some specific temperatures higher than 380K corresponding to transition phenomena in PMMA where a decrease of $(-\Delta G_a^p(T)$ against the coverage rate was observed. The same variations were found for the various adsorbed polar solvents.

The curves of $(-\Delta G_a^p(T)$ of the different solvents plotted in Figures S1–S7 clearly showed the large effect of the temperature on the polar free energy with non linear variations in the case of PMMA in bulk phase and when adsorbed on silica at different recovery fractions. This non-linearity of $(-\Delta G_a^p(T)$ was essentially observed near the transition temperatures of PMMA that were respectively highlighted at 333.15K, 383.15 and 433.15K, whereas, the linearity was shown far from these transition temperatures. However, for all solvents, the linearity $(-\Delta G_a^p(T)$ was assured for silica particles with an excellent linear regression coefficient very close to 1.000. It was also showed in Figures S1–S7 that the variations of $(-\Delta G_a^p(T))$ for the different coverage rates until the monolayer were in general limited between the two curves representative of PMMA in bulk phase and of silica particles with the results of monolayer approaching that of PMMA showing a mask effect exerted by PMMA on silica particles and limiting the role of silica on the interaction between the polar molecules and the solid surfaces.

To determine the polar enthalpy $(-\Delta H_a^p(T))$ and entropy $(-\Delta S_a^p(T))$ of interaction between solvents and composites, relations (8) and (9) were applied on the non-linear variations of $(-\Delta G_a^p(T)$ of adsorbed polar solvents by taking small parabolic portions of the representative curves. The values of $(-\Delta H_a^p(T))$ and $(-\Delta S_a^p(T))$ were given in Tables S4–S8. An important difference in the behavior of the various solid surfaces was shown in Tables S4–S8 strongly depending on the temperature and on the coverage rate. To highlight the important effect of the temperature and the adsorption of PMMA on silica particles, the results were plotted on Figures 8–12 giving the curves of the enthalpy $(-\Delta H_a^p(T))$ and entropy $(-\Delta S_a^p(T))$ of polar solvents adsorbed on the various solid substrates as a

 doi:10.20944/preprints202403.0997.v1

function of the temperature by varying the coverage rate of the adsorption of PMMA on silica. The results in Figure 8 concerning the silica particles were plotted independently from the temperature; indeed, a perfect linearity was observed in the variations of the free polar energy $(-\Delta G_a^p(T)$ of all adsorbed polar molecules and constants values of $(-\Delta H_a^p)$ and $(-\Delta S_a^p)$ were obtained in the case of silica particles (Figure 8, Table S8).

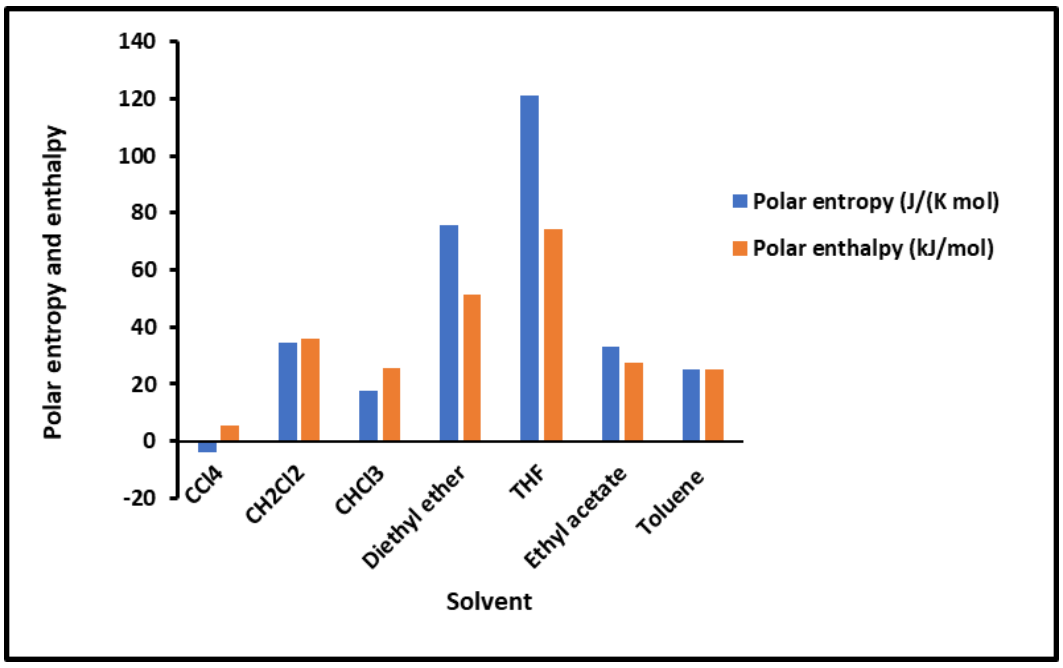

Figure 8. Values of the interaction enthalpy ($-\Delta H_a^p(T)\ (kJ/mol)$) and entropy $(-\Delta S_a^p(T)\ (JK^{-1}mol^{-1}))$ of polar solvents adsorbed on silica independent from the temperature.

However, the curves obtained with the various polymers PMMA in bulk and/or adsorbed phases plotted in Figures 9–12 showed an extreme non-linearity variations of $(-\Delta H_a^p(T))$ and entropy $(-\Delta S_a^p(T))$ versus the temperature.

An intersting and original result was noted by the varaitions of polar enethalpy and entropy given in Figures 9–12, showing four minima of the various curves mentioning specific and particular temperatures. In previous papers [], three transition temperatures were observed with PMMA and PMMA/silica at different coverages of PMMA on the silica particles respectively related to beta-relaxation $(T_\beta = 60°C)$, glass transition $(T_g = 110°C)$ and other liquid-liquid transition $(T_{liq-liq} = 160°C)$. A shift of these transition temperatures was observed in the case of the adsorption of PMMA on metallic oxides reaching 20°C when PMMA is adsorbed on silica.

Preprints.org (www.preprints.org) | NOT PEER-REVIEWED | Posted: 18 March 2024 doi:10.20944/preprints202403.0997.v1

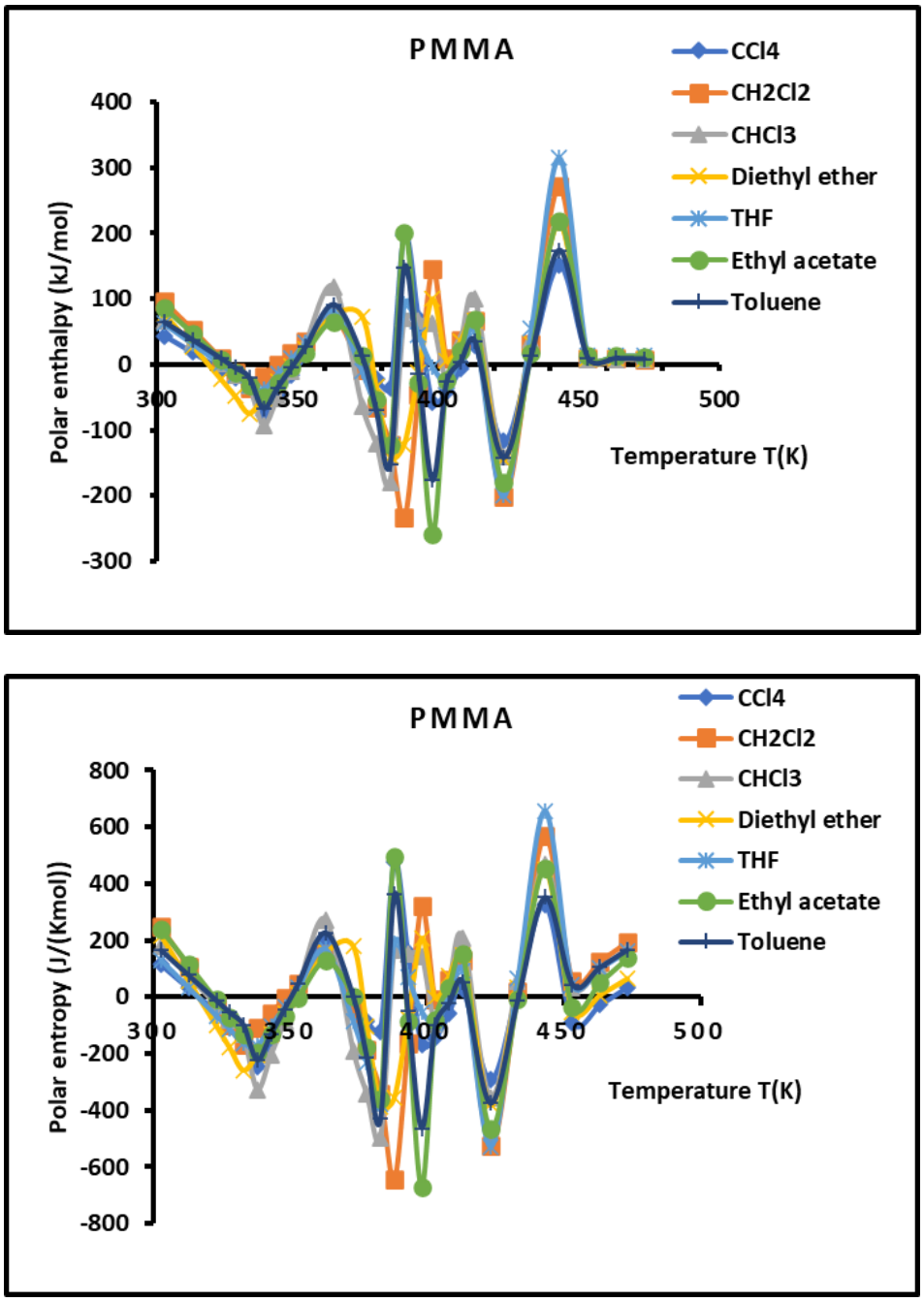

Figure 9. Variations of the interaction enthalpy ($-\Delta H_a^p(T))\ (kJ/mol)$ and entropy $(-\Delta S_a^p(T))\ (JK^{-1}mol^{-1})$ of polar solvents adsorbed on PMMA as a function of the temperature.

In this work, four temperatures in the case of PMMA were noted: $T_\beta = 338.15K$, $T_g = 383.15K$, $T_3 = 398.15K$ and $T_{liq-liq} = 423.15K$ (Figure 10, Table S4). The three previous transition temperatures were then confirmed by this study. However, the presence of a fourth temperature $T_3 = 398.15K$ in the case of bulk PMMA deserves more thought.

In the case of composite PMMA/silica with a coverage rate $\theta = 0.31$, there are other shifted values of the transition temperatures. The new values are the following $T_\beta = 333.15K$, $T_g = 373.15K$, $T_3 = 398.15K$ and $T_{liq-liq} = 443.15K$ (Figure 11, Table S5). It seems that this recovery fraction increases the liquid-liquid transition temperature about 20°C with a decrease of the glass transition about 10°C relatively to PMMA in bulk phase.

Preprints.org (www.preprints.org) | NOT PEER-REVIEWED | Posted: 18 March 2024 doi:10.20944/preprints202403.0997.v1

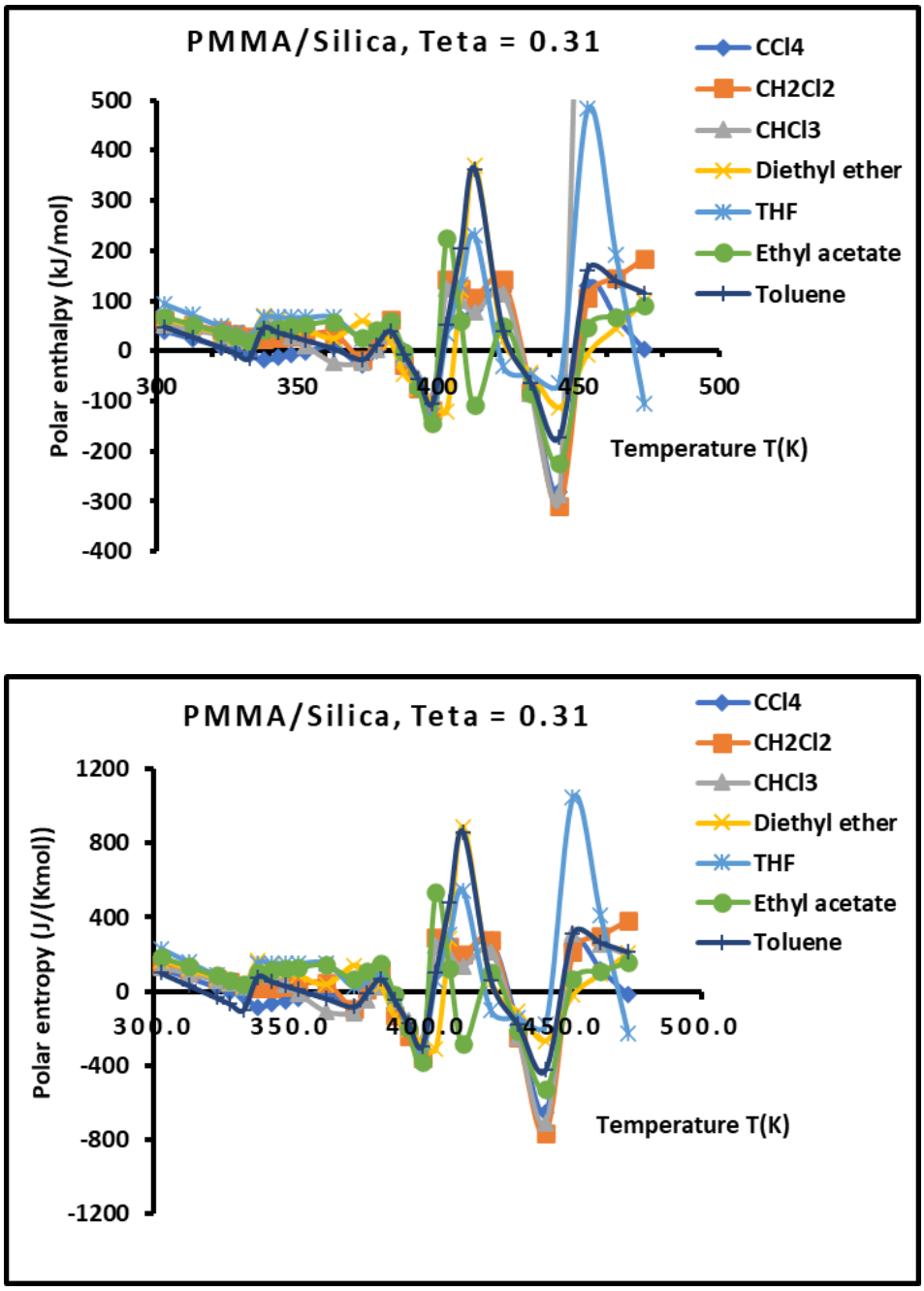

Figure 10. Variations of the interaction enthalpy ($-\Delta H_a^p(T))\ (kJ/mol)$ and entropy $(-\Delta S_a^p(T))\ (JK^{-1}mol^{-1})$ of polar solvents adsorbed on PMMA/silica for $\theta = 0.31$ as a function of the temperature.

For a coverage fraction $\theta = 0.83$, the reported values are $T_\beta = 333.15K$, $T_g = 383.15K$, $T_3 = 403.15K$ and $T_{liq-liq} = 423.15K$. the same values of PMMA in bulk phase were observed with small variation of 5°C for T_β and T_3 (Figure 11, Table S6)

However, for the case of one monolayer of PMMA on silica, identical values of transition temperatures of bulk PMMA were noted showing that the composite behavior of a monolayer is identical to that of PMMA in bulk phase (Figure 12, Table S7).

Preprints.org (www.preprints.org) | NOT PEER-REVIEWED | Posted: 18 March 2024 doi:10.20944/preprints202403.0997.v1

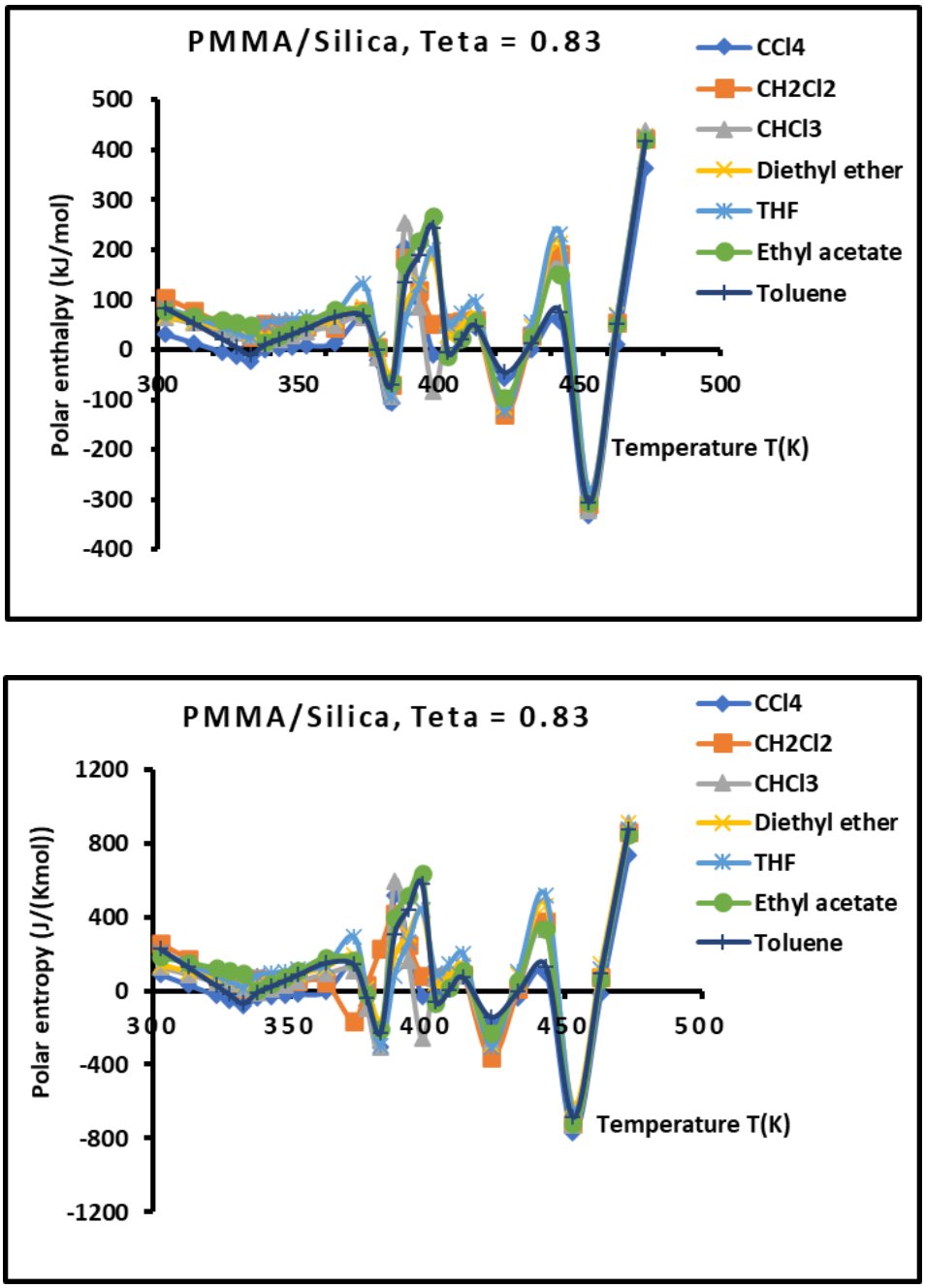

Figure 11. Variations of the interaction enthalpy ($-\Delta H_a^p(T))\ (kJ/mol)$ and entropy $(-\Delta S_a^p(T))\ (JK^{-1}mol^{-1})$ of polar solvents adsorbed on PMMA/silica for $\theta = 0.83$ as a function of the temperature.

Preprints.org (www.preprints.org) | NOT PEER-REVIEWED | Posted: 18 March 2024 doi:10.20944/preprints202403.0997.v1

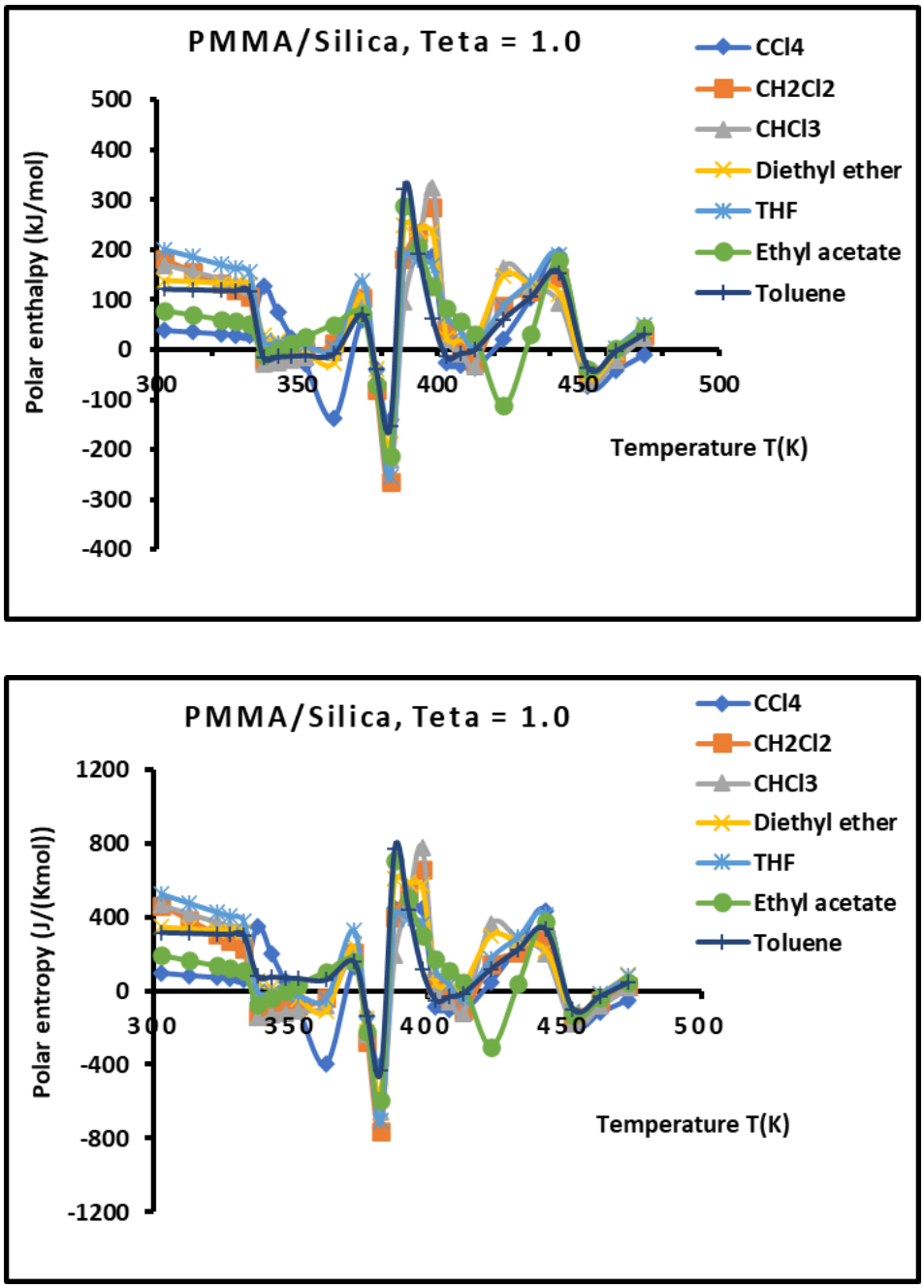

Figure 12. Variations of the interaction enthalpy ($-\Delta H_a^p(T))\ (kJ/mol)$ and entropy $(-\Delta S_a^p(T))\ (JK^{-1}mol^{-1})$ of polar solvents adsorbed on PMMA/silica for $\theta = 1.0$ (monolayer case) as a function of the temperature.

3.3. Enthalpic and Entropic Lewis's Acid-Base Parameters

The variations of the interaction enthalpy $(-\Delta H_a^p(T))$ and entropy $(-\Delta S_a^p(T))$ of the various polar molecules adsorbed on the different solid surfaces were given in Tables S4 to S8 and plotted on Figures 8–12. These results were used with relations 10 and 11 to determine the variations of the enthalpic acid base parameters K_A and K_D and the entropic acid base parameters ω_A and ω_D of PMMA and PMMA/silica at different recovery fractions as a function of the temperature. The calculated values of the acid-base parameters functions of the temperature for the different solid surfaces were given in Table 6–9. The obtained results showed an important variation of the different acid-base parameters of PMMA and the composites PMMA/silica as a function of the temperature and coverage rate of the system PMMA/silica. The results in Table 6 showed that PMMA exhibited

 doi:10.20944/preprints202403.0997.v1

higher basic surface (about 8 to 10 times more basic than acidic) and lower acid character about half of that found with the silica particles (Table 10). However, the acid-base character of PMMA strongly with the increase of the temperature with sudden changes near the transition temperatures with negative values of the acid-base parameters around the transition temperature, certainly due to the variation of chemical group conformations in PMMA. Figures S8 to S11 also showed three to four secondary minima reflecting the presence of transition temperatures in PMMA and PMMA/silica systems. Figures S8 to S15 clearly showed the sudden variations of the acid-base parameters near the transition temperatures and also confirmed these transition phenomena in the different composites PMMA/silica. It was observed that the acidity of PMMA/silica sightly varied when the recovery fraction increases from $\theta = 0$ to $\theta = 0.83$, whereas, the basicity globally increases when the recovery fraction increases (Tables 6–9 and Figures S8–S15). However, the results in Table 9 and Figure S11 gave higher acid-base parameters in the case of the monolayer of PMMA on silica relatively to silica particles and bulk PMMA. This special case of specific adsorption will probably create more surface chemical groups increasing the number of acidic and basic groups in Lewis terms at the surface of PMMA/silica that implies an increase of the Lewis acid-base parameters of adsorbed PMMA on silica.

Table 6. Values of the enthalpic acid base parameters K_A, K_D, K_D/K_A and $K_D + K_A$, and the entropic acid base parameters ω_A , ω_D, ω_D / ω_A and $(\omega_D + \omega_A)$ of PMMA as a function of the temperature.

T(K)	K_A	K_D	$K_D + K_A$	K_D/K_A	$10^3.\omega_A$	$10^3.\omega_D$	$10^3(\omega_D + \omega_A)$	ω_D / ω_A
303.15	0.478	3.881	4.358	8.120	0.90	18.20	19.10	20.15
313.15	0.317	2.523	2.840	7.953	0.56	7.52	8.08	13.40
323.15	0.090	0.664	0.754	7.413	-0.62	-3.15	-3.77	5.12
328.15	-0.122	-0.522	-0.644	4.293	-1.00	-4.91	-5.90	4.93
333.15	-0.153	-0.636	-0.789	4.160	-1.38	-6.06	-7.44	4.41
338.15	-0.144	-0.658	-0.802	4.568	-0.88	-7.59	-8.47	8.63
343.15	0.152	-0.695	-0.543	-4.565	-0.59	-8.31	-8.91	14.04
348.15	0.170	-0.529	-0.358	-3.103	-0.16	-1.87	-2.03	11.61
353.15	0.278	1.826	2.105	6.560	0.20	2.78	2.98	14.04
363.15	0.536	3.122	3.658	5.828	0.92	15.67	16.59	17.10
373.15	0.433	3.955	4.388	9.135	0.90	7.40	8.30	8.24
378.15	0.398	3.739	4.138	9.385	-1.99	-8.98	-10.97	4.52
383.15	0.186	1.527	1.713	8.217	-0.66	-6.52	-7.19	9.84
388.15	0.521	5.841	6.362	11.213	0.91	12.80	13.71	14.05
393.15	0.274	1.750	2.024	6.389	0.29	2.47	2.76	8.42
398.15	0.266	0.560	0.826	2.106	0.27	-1.89	-1.62	-6.93
403.15	0.220	-0.630	-0.410	-2.864	-0.45	-1.32	-1.77	2.92
408.15	0.174	0.800	0.975	4.595	0.22	-0.66	-0.44	-2.95
413.15	0.433	3.358	3.791	7.755	0.90	6.21	7.10	6.91
423.15	0.488	2.131	2.619	4.366	-4.56	-14.72	-19.27	3.23
433.15	0.543	0.904	1.447	1.665	0.66	-0.40	0.26	-0.61
443.15	1.755	7.262	9.016	4.138	5.88	19.88	25.76	3.38
453.15	0.111	1.044	1.155	9.419	0.60	-1.83	-1.22	-3.04
463.15	0.107	1.047	1.154	9.766	1.00	1.60	2.61	1.60
473.15	0.100	0.980	1.080	9.832	1.40	6.23	7.63	4.44

 doi:10.20944/preprints202403.0997.v1

Table 7. Values of the enthalpic acid base parameters K_A, K_D, K_D/K_A and $K_D + K_A$, and the entropic acid base parameters ω_A , ω_D, ω_D / ω_A and $(\omega_D + \omega_A)$ of PMMA/silica for $\theta = 0.31$ as a function of the temperature.

T(K)	K_A	K_D	$K_D + K_A$	K_D/K_A	$10^3.\omega_A$	$10^3.\omega_D$	$10^3(\omega_D + \omega_A)$	ω_D / ω_A
303.15	0.884	3.819	4.704	4.318	2.11	10.71	12.82	5.06
313.15	0.704	2.319	3.023	3.291	1.53	5.84	7.37	3.81
323.15	0.519	0.770	1.288	1.484	0.95	0.97	1.91	1.02
328.15	0.424	-0.023	0.400	-0.055	0.65	-0.52	0.14	-0.79
333.15	0.327	-0.828	-0.501	-2.532	0.36	-0.73	-0.37	-2.02
338.15	0.789	0.508	1.298	0.644	1.97	-0.94	1.03	-0.48
343.15	0.781	0.387	1.168	0.495	1.95	-1.19	0.76	-0.61
348.15	0.773	0.264	1.037	0.341	1.92	-1.20	0.72	-0.63
353.15	0.764	0.139	0.903	0.181	1.90	-1.34	0.56	-0.71
363.15	0.747	-0.117	0.630	-0.157	1.85	-1.67	0.19	-0.90
373.15	2.013	2.013	4.026	1.000	4.85	15.21	20.05	3.14
378.15	0.425	0.594	1.020	1.397	0.84	-0.56	0.28	-0.67
383.15	0.781	0.387	1.168	0.495	1.95	-0.73	1.21	-0.38
388.15	-0.530	-1.038	-1.568	1.959	-0.57	-2.05	-2.62	3.61
393.15	-0.717	-1.493	-2.210	2.083	-1.54	-3.12	-4.66	2.03
398.15	-0.917	-2.588	-3.505	2.821	-2.39	-3.21	-5.60	1.34
403.15	0.584	7.647	8.231	13.084	-3.52	12.57	9.05	-3.58
408.15	1.006	11.211	12.216	11.149	2.39	18.37	20.76	7.67
413.15	2.013	14.818	16.831	7.362	4.85	21.18	26.03	4.37
423.15	-2.076	9.053	6.977	-4.361	-3.51	13.30	9.79	-3.79
433.15	-0.729	-2.522	-3.250	3.460	-1.26	-1.61	-2.87	1.27
443.15	0.550	-1.493	-0.944	-2.718	0.99	-1.72	-0.73	-1.74
453.15	4.266	9.254	13.520	2.169	10.38	-1.11	9.27	-0.11
463.15	1.213	15.550	16.763	12.821	3.76	10.71	14.47	2.84
473.15	-1.907	14.815	12.908	-7.768	-2.85	10.46	7.61	-3.67

Table 8. Values of the enthalpic acid base K_A, K_D, K_D/K_A and $K_D + K_A$, and the entropic acid base parameters ω_A , ω_D, ω_D / ω_A and $(\omega_D + \omega_A)$ of PMMA/silica for $\theta = 0.83$ as a function of the temperature.

T(K)	K_A	K_D	$K_D + K_A$	K_D/K_A	$10^3.\omega_A$	$10^3.\omega_D$	$10^3(\omega_D + \omega_A)$	ω_D / ω_A
303.15	0.736	5.459	6.195	7.421	1.73	14.24	15.97	8.23
313.15	0.621	3.385	4.006	5.448	1.36	7.51	8.86	5.52
323.15	0.503	1.243	1.747	2.471	0.99	0.77	1.76	0.78
328.15	0.443	0.147	0.590	0.333	0.80	-1.40	-0.60	-1.74
333.15	0.381	-0.966	-0.584	-2.531	0.62	-1.92	-1.31	-3.12
338.15	0.579	-0.169	0.410	-0.292	1.07	-2.54	-1.47	-2.37
343.15	0.605	0.520	1.125	0.860	1.15	-1.89	-0.74	-1.64
348.15	0.632	1.220	1.851	1.931	1.23	-0.28	0.94	-0.23
353.15	0.659	1.929	2.588	2.929	1.30	1.74	3.04	1.33

 doi:10.20944/preprints202403.0997.v1

363.15	0.714	3.379	4.093	4.732	1.46	5.79	7.24	3.97
373.15	0.893	3.854	4.747	4.316	1.91	0.69	2.60	0.36
378.15	0.315	-1.651	-1.336	-5.240	0.30	-0.70	-0.40	-2.34
383.15	0.605	0.520	1.125	0.860	1.15	2.31	3.46	2.01
388.15	0.778	22.143	22.921	28.465	-2.56	13.14	10.57	-5.12
393.15	0.962	14.877	15.839	15.464	1.76	12.13	13.89	6.90
398.15	2.200	7.518	9.718	3.417	4.89	11.61	16.50	2.38
403.15	0.595	-1.252	-0.657	-2.105	1.18	-2.16	-0.99	-1.84
408.15	0.743	1.285	2.028	1.730	1.54	0.41	1.95	0.27
413.15	0.893	3.854	4.747	4.316	1.91	6.66	8.57	3.50
423.15	-1.125	-1.531	-2.656	1.361	-1.46	-2.53	-3.99	1.74
433.15	0.602	0.223	0.824	0.370	1.38	-1.26	0.12	-0.91
443.15	2.369	6.543	8.912	2.762	5.41	10.87	16.28	2.01
453.15	-1.704	-4.480	-6.185	2.629	-2.26	-4.54	-6.80	2.01
463.15	0.679	2.897	3.577	4.264	1.26	2.74	4.00	2.18
473.15	4.310	23.213	27.523	5.386	2.06	2.73	4.80	1.33

Table 9. Values of the enthalpic acid base parameters K_A, K_D, K_D/K_A and $K_D + K_A$, and the entropic acid base parameters ω_A , ω_D, ω_D / ω_A and $(\omega_D + \omega_A)$ of PMMA/silica for $\theta = 1.0$ as a function of the temperature.

T(K)	K_A	K_D	$K_D + K_A$	K_D/K_A	$10^3.\omega_A$	$10^3.\omega_D$	$10^3(\omega_D + \omega_A)$	ω_D / ω_A
303.15	2.135	6.006	8.141	2.813	5.06	14.99	20.06	2.96
313.15	1.805	5.719	7.524	3.169	4.61	14.06	18.67	3.05
323.15	1.661	5.423	7.084	3.266	4.16	13.13	17.29	3.16
328.15	1.587	5.272	6.859	3.322	3.93	12.67	16.60	3.22
333.15	1.512	5.118	6.630	3.385	3.70	12.20	15.90	3.30
338.15	2.177	6.179	8.357	2.838	-2.30	15.92	13.62	-6.92
343.15	0.385	3.423	3.808	8.884	-3.19	12.37	9.19	-3.88
348.15	0.452	0.627	1.078	1.388	-2.59	4.01	1.42	-1.55
353.15	0.510	-1.015	-0.506	-1.992	0.51	4.36	4.87	8.54
363.15	0.611	-1.645	-1.035	-2.695	0.75	13.22	13.96	17.68
373.15	0.385	-0.996	-0.611	-2.585	0.45	6.65	7.10	14.73
378.15	-0.439	-0.731	-1.169	1.666	-2.86	11.09	8.23	-3.88
383.15	-0.735	3.423	2.688	-4.659	-2.31	9.21	6.90	-3.99
388.15	1.235	21.076	22.312	17.060	2.59	19.86	22.46	7.66
393.15	1.188	18.884	20.072	15.892	2.47	21.30	23.78	8.61
398.15	1.141	13.057	14.197	11.448	2.35	18.65	21.01	7.93
403.15	0.887	-1.004	-0.117	-1.132	1.64	-1.93	-0.29	-1.17
408.15	0.558	-0.941	-0.383	-1.687	0.83	-1.86	-1.03	-2.25
413.15	0.224	-0.452	-0.228	-2.017	0.73	-1.81	-1.08	-2.49
423.15	0.786	2.985	3.771	3.798	1.57	4.81	6.38	3.08
433.15	1.060	9.697	10.756	9.149	2.21	13.41	15.62	6.08
443.15	1.340	13.578	14.918	10.131	2.85	15.73	18.58	5.53

 doi:10.20944/preprints202403.0997.v1

453.15	-1.978	6.298	4.320	-3.184	-1.53	-1.92	-3.46	1.26
463.15	0.188	-0.611	-0.422	-3.242	0.23	-0.74	-0.51	-3.25
473.15	0.571	1.133	1.703	1.985	1.04	-0.74	0.31	-0.71

On the contrary, the case of silica gave acid-base parameters independent from the temperature (Table 10) and showed higher acid character than that of the other PMMA/silica surfaces.

Table 10. Values of the enthalpic acid base parameters K_A, K_D, K_D/K_A and $K_D + K_A$, and the entropic acid base parameters ω_A , ω_D, ω_D / ω_A and $(\omega_D + \omega_A)$ of silica.

Solid surface	K_A	K_D	$K_D + K_A$	K_D/K_A	$10^3.\omega_A$	$10^3.\omega_D$	$10^3(\omega_D + \omega_A)$	ω_D / ω_A
Silica	0.807	0.412	1.219	0.510	1.39	-1.32	0.07	-0.95

3.4. London Dispersive Free Interaction Energies of PMMA/silica

The new method applied in this paper and based on the London dispersive energy of interaction allowed to determine the London dispersive free energies of adsorbed solvents on the composites PMMA/silica at different recovery fractions and temperatures by using the following London dispersion interactions.

$$\Delta G_a^d(T) = A\left[\frac{3\mathcal{N}}{2(4\pi\varepsilon_0)^2}\mathcal{P}_{SX}\right] \quad (12)$$

The dispersion factor A was obtained by applying equation 5 on the n-alkanes adsorbed on the various composite materials. The results were given in Table 11 and Figures 13 and 14 which irrevocably showed the presence of several transition temperatures located at the various maxima (in bold on Table 11) of the dispersion factor.

The values of the transition temperatures are identical to those previously obtained in this work and other studies. The adsorption of PMMA on silica is characterized by transition temperature shift in the case of a recovery fraction $\theta = 0.31$. It was shown on Figure 14 that the limit of the dispersion factor was obtained for PMMA in bulk phase (then for a recovery fraction $\theta \geq 2$.

Table 11. Values of the dispersion factor A of the various PMMA/silica as a function of the temperature. The maxima of A are represented in bold.

T(K)	Silica, $\theta = 0$	PMMA/silica, $\theta = 0.31$	PMMA/silica, $\theta = 0.83$	PMMA/silica, $\theta = 1.0$	PMMA
303.15	378.20	395.51	354.74	337.33	297.06
313.15	367.18	371.55	340.26	319.84	276.45
323.15	356.15	353.99	319.89	299.94	268.35
328.15	350.64	348.49	327.15	308.07	274.64
333.15	345.13	353.01	**340**	**322.86**	**296.16**
338.15	339.62	357.02	330.02	310.12	272.62
343.15	334.11	**361.76**	317.89	297.17	257.28
348.15	328.60	341.88	304.58	284.75	245.91
353.15	323.09	322.53	289.18	272.25	237.62
363.15	312.07	296.06	266.8	250.08	227
373.15	301.04	271.64	237.43	219.87	231.39
378.15	295.53	266.5	229.4	215.81	262.31
383.15	290.02	263.87	248.84	267.22	**307.3**
388.15	284.51	271.09	**302.26**	**317.52**	252.09
393.15	279.00	290.69	274.76	296.44	221.75
398.15	273.49	**311.45**	256.56	272.99	209.51

 doi:10.20944/preprints202403.0997.v1

403.15	267.98	291.54	242.31	238.62	199.78
408.15	262.47	268.3	222.02	215.57	196.16
413.15	256.96	247.67	202.81	198.03	193.27
423.15	245.93	233.94	196.97	194.06	215.82
433.15	234.91	238.92	**231.59**	**226.19**	**258.37**
443.15	223.89	**241.02**	192.79	180.85	195.77
453.15	212.87	214.66	175.48	156.95	166.58
463.15	201.85	206.05	168.88	150.69	158.53
473.15	190.82	180.38	146.81	131.75	136.51

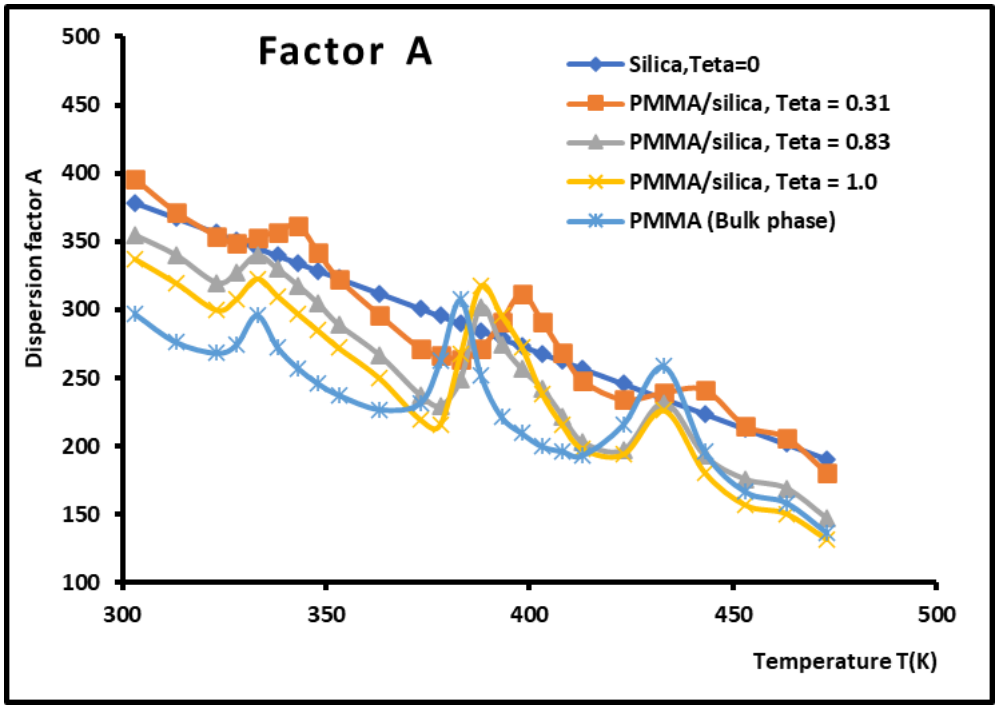

Figure 13. Variations of the dispersion factor *A* (SI unit) of PMMA/silica at different recovery fractions as a function of the temperature.

 doi:10.20944/preprints202403.0997.v1

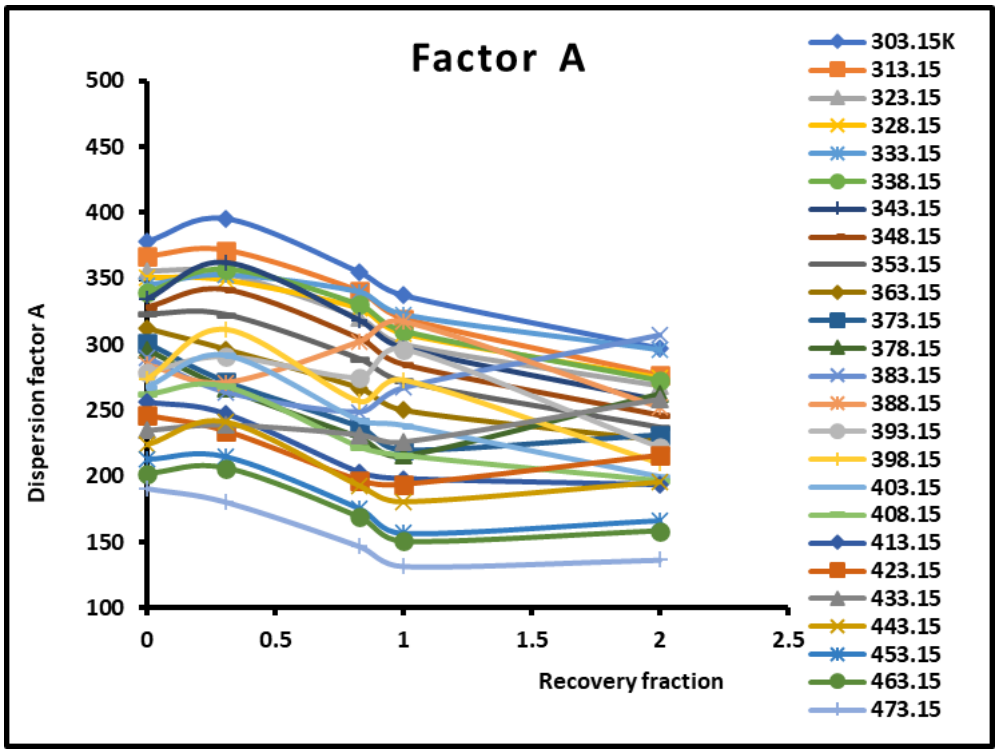

Figure 14. Variations of the dispersion factor A (SI unit) of different solid surfaces as a function of the recovery fraction for different temperatures.

The determination of the dispersion factor of the various PMMA/silica allowed giving in Tables S9–S11 the London dispersive energy of adsorption of the various organic solvents on PMMA (bulk phase) and PMMA/silica at different recovery fractions and temperatures. The transition temperatures were also highlighted in Tables S9–S11. Figure 15 gave an example of the variations of the London dispersive energy in the case of adsorption of PMMA on silica with $\theta = 0.83$. The same previous conclusions concerning the presence of the transition temperatures were observed for a recovery fraction of 31% of PMMA on silica.

 doi:10.20944/preprints202403.0997.v1

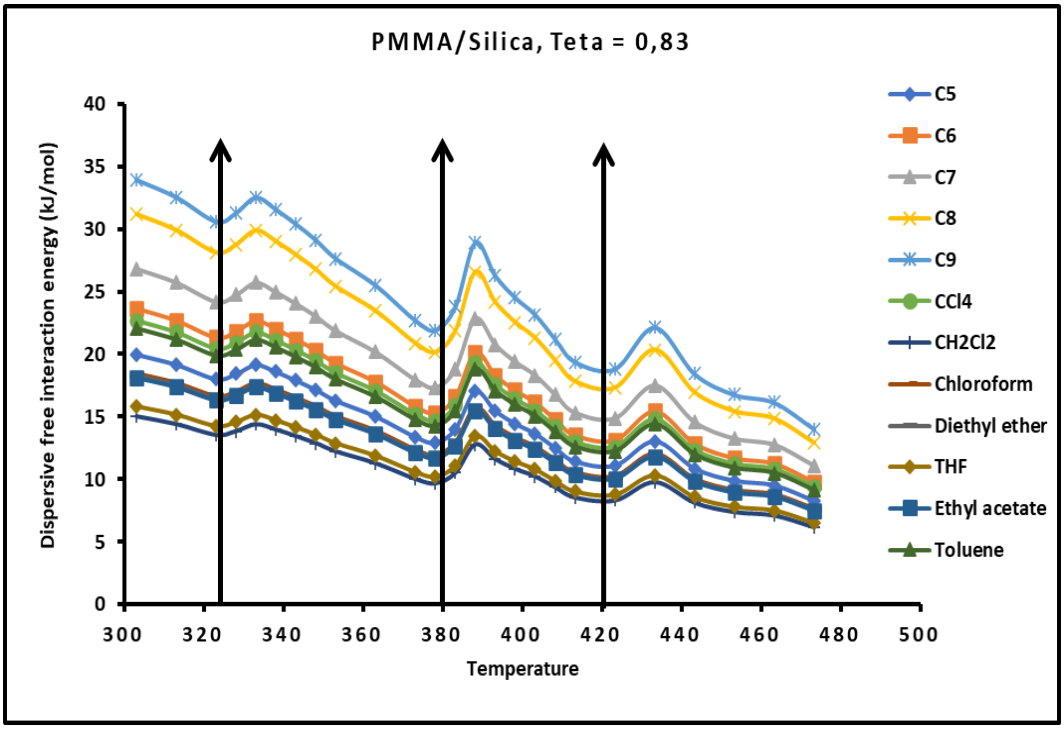

Figure 15. Evolution of the London free dispersive interaction energy $(-\Delta G_a^d(T)$ of organic solvents adsorbed on PMMA/silica for $\theta = 0.31$ as a function of the temperature.

3.5. Determination of the Separation Distance H between Solid Particles and Solvents

The average separation distance H between the adsorbed solvents and the various solid surfaces was calculated by using the experimental results and relations 5 and 6. The variations of H as a function of the temperature for the various solid substrates were plotted on Figure 16.

It was observed that the variations of the separation H depends on the temperature, the nature of the solid surface and the recovery fraction. H increased when the temperature increased. This is conformed with the kinetic theory and the thermal agitation that has the increase effect of the separation distance between particles.

The larger separation H was found between silica particles and solvents, while the closest distance was obtained for a recovery fraction $\theta = 0.31$ of PMMA adsorbed on silica. When comparing the curves of Figures 15 and 16, it was noted that for $\theta = 0.31$, the minimum of the dispersive energy corresponds to a maximum of the separation distance. Indeed, the minimum of attractive energy is necessary equivalent to the higher separation distance. Once again, the curves of Figure 16 showed the presence of maxima at the transition temperatures.

 doi:10.20944/preprints202403.0997.v1

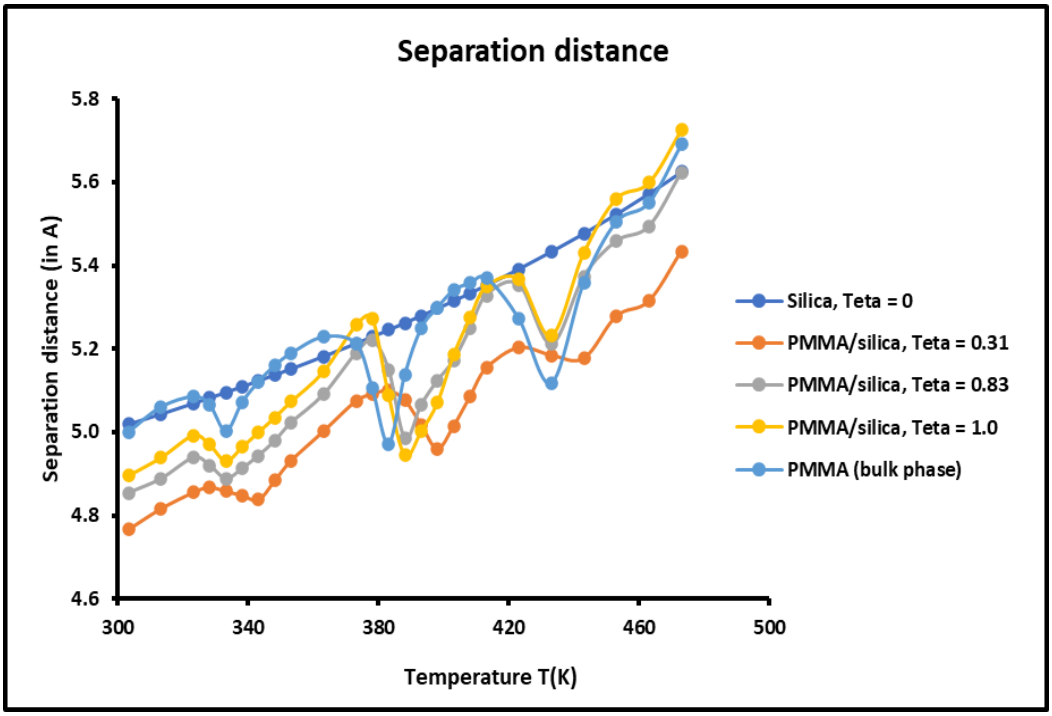

Figure 16. Variations of the separation distance H as a function of the temperature for the different solid surfaces.

4. Conclusions

A new methodology was proposed to study the physicochemical properties of the composites constituted by the adsorption of PMMA on silica particles with various coverage rates between $\theta = 0$ (case of silica) and $\theta = 1$ corresponding to a monolayer. The inverse gas chromatography at infinite dilution was used by applying the London dispersion interaction energy to separate the polar and dispersive energy of adsorbed solvents on the different solid surfaces. A new intrinsic thermodynamic parameter including the deformation polarizability of solvents and the harmonic mean of the ionization energies of solid surface and organic molecules. The determination of the polar interaction energy $\Delta G_a^p(T)$ as a function of the temperature relative to the various composites PMMA/silica let to the values of the polar enthalpy and entropy. It was showed that all polar surface variables depended on the temperature and the coverage rates of PMMA adsorbed on silica particles.

The Lewis enthalpic and entropic acid-base parameters were determined for the various solid surfaces. All acid-base parameters of PMMA and PMMA/silica were found strongly dependent on the temperature. Only those of silica particles did not depend on the temperature. Silica exhibited higher acidic surface (twice more acidic than basic), whereas, the acid-base parameters of PMMA in bulk phase showed higher basic character varying as a function of the temperature (8 times more basic than acid in general). The acidity of the composites PMMA/silica slightly varied versus the temperature relatively to the highest values of Lewis basic parameters. However, the basicity of PMMA/silica increased with the recovery fraction to reach a maximum for a monolayer of adsorption. It seemed that the acidity of PMMA/silica for a monolayer reached the highest value.

The variations of the different thermodynamic and physicochemical parameters showed secondary minima and maxima highlighting the presence of several transition temperature for PMMA in bulk phase and for the systems PMMA/silica with different recovery fractions with a shift of such temperatures in the case of a recovery fraction equal to 31%

This new study also determined the average separation distance between the organic solvents and the various solid surfaces. It was showed that the separation distance is comprised between 4 Å and 7 Å. It was observed a slight variation of the intermolecular distance as a function of the temperature and the recovery fraction of PMMA on silica particles.

 doi:10.20944/preprints202403.0997.v1

Supplementary Materials: The following supporting information can be downloaded at the website of this paper posted on Preprints.org, Table S1. Values of deformation polarizability and ionization energy of n-alkanes and polar molecules. Table S2. Values of the harmonic mean of the ionization energies $\frac{\varepsilon_S\,\varepsilon_X}{(\varepsilon_S+\,\varepsilon_X)}$ of silica and organic solvents and the parameter $\frac{3\mathcal{N}}{2(4\pi\varepsilon_0)^2}\mathcal{P}_{S-X}$ for the various organic molecules. Table S3. Values of the harmonic mean of the ionization energies $\frac{\varepsilon_S\,\varepsilon_X}{(\varepsilon_S+\,\varepsilon_X)}$ of PMMA and organic solvents and the parameter $\frac{3\mathcal{N}}{2(4\pi\varepsilon_0)^2}\mathcal{P}_{S-X}$ for the various organic molecules. Figure S1. Variations of the polar free interaction energy of CCl4 adsorbed on PMMA/silica a function of the temperature, at different recovery fractions. Figure S2. Variations of the polar free interaction energy of CH2Cl2 adsorbed on PMMA/silica a function of the temperature, at different recovery fractions. Figure S3. Variations of the polar free interaction energy of CHCl3 adsorbed on PMMA/silica as a function of the temperature, at different recovery fractions. Figure S4. Variations of the polar free interaction energy of diethyl ether adsorbed on PMMA/silica as a function of the temperature, at different recovery fractions. Figure S5. Variations of the polar free interaction energy of THF adsorbed on PMMA/silica as a function of the temperature, at different recovery fractions. Figure S6. Variations of the polar free interaction energy of ethyl acetate adsorbed on PMMA/silica as a function of the temperature, at different recovery fractions. Figure S7. Variations of the polar free interaction energy of toluene adsorbed on PMMA/silica as a function of the temperature, at different recovery fractions. Table S4. Values (in kJ/mol) of polar enthalpy $(-\Delta H_a^p(T)$ and $(-\Delta S_a^p(T)$ of polar solvents adsorbed on PMMA particles at different temperatures. Table S5. Values (in kJ/mol) of polar enthalpy $(-\Delta H_a^p(T)$ and $(-\Delta S_a^p(T)$ of polar solvents adsorbed on PMMA/silica particles at different temperatures for a recovery fraction of 31%. Table S6. Values (in kJ/mol) of polar enthalpy $(-\Delta H_a^p(T)$ and $(-\Delta S_a^p(T)$ of polar solvents adsorbed on PMMA/silica for $\theta = 0.83$ at different temperatures. Table S7. Values (in kJ/mol) of polar enthalpy $(-\Delta H_a^p(T)$ and $(-\Delta S_a^p(T)$ of polar solvents adsorbed on PMMA/silica for $\theta = 1.0$ (monolayer) at different temperatures. Table S8. Values (in kJ/mol) of polar enthalpy $(-\Delta H_a^p(T)$ and $(-\Delta S_a^p(T)$ of polar solvents adsorbed on silica particles at different temperatures. Figure S8. Evolutions of the enthalpic acid base parameters K_A, K_D, K_D/K_A and $K_D + K_A$, and the entropic acid base parameters ω_A , ω_D, ω_D / ω_A and $(\omega_D + \omega_A)$ of PMMA as a function of the temperature. Figure S9. Evolutions of the enthalpic acid base parameters K_A, K_D, K_D/K_A and $K_D + K_A$, and the entropic acid base parameters ω_A , ω_D, ω_D / ω_A and $(\omega_D + \omega_A)$ of PMMA/silica for $\theta = 0.31$ as a function of the temperature. Figure S10. Evolutions of the enthalpic acid base parameters K_A, K_D, K_D/K_A and $K_D + K_A$, and the entropic acid base parameters ω_A , ω_D, ω_D / ω_A and $(\omega_D + \omega_A)$ of PMMA/silica for $\theta = 0.83$ as a function of the temperature. Figure S11. Evolutions of the enthalpic acid base parameters K_A, K_D, K_D/K_A and $K_D + K_A$, and the entropic acid base parameters ω_A , ω_D, ω_D / ω_A and $(\omega_D + \omega_A)$ of PMMA/silica for $\theta = 1.0$ as a function of the temperature. Figure S12. Evolutions of the enthalpic Lewis acid parameter K_A as a function of the recovery fraction and temperature. Figure S13. Evolutions of the enthalpic Lewis basic parameter K_D as a function of the recovery fraction and temperature. Figure S14. Evolutions of the entropic Lewis acidic parameter ω_A as a function of the recovery fraction and temperature. Figure S15. Evolutions of the entropic Lewis basic parameter ω_D as a function of the recovery fraction and temperature. Table S9. Values (in kJ/mol) of the London free dispersive interaction energy $(-\Delta G_a^d(T)$ of organic solvents adsorbed on PMMA at different temperatures. Table S10. Values (in kJ/mol) of the London free dispersive interaction energy $(-\Delta G_a^d(T)$ of organic solvents adsorbed on PMMA/silica for $\theta = 0.31$ at different temperatures. Table S11. Values (in kJ/mol) of the London free dispersive interaction energy $(-\Delta G_a^d(T)$ of organic solvents adsorbed on PMMA/silica for $\theta = 0.83$ at different temperatures. Table S12. Values (in kJ/mol) of the London free dispersive interaction energy $(-\Delta G_a^d(T)$ of organic solvents adsorbed on PMMA/silica for $\theta = 1.0$ (monolayer) at different temperatures.

Funding: This research did not receive any specific grant.

Data Availability Statement: There is no additional data.

Conflicts of Interest: The author declares no conflict of interest.

References

1. Mathur, S.; Moudgil, B.M. Mechanisms of nonionic polymer adsorption on oxide surfaces. *Mining, Metallurgy & Exploration*, **1998**, 15, 24–28. https://doi.org/10.1007/BF03402794
2. Jimenez, A.M.; Zhao, D.; Misquitta, K.; Jestin, J.; Kumar, S.K. Exchange lifetimes of the bound polymer layer on silica nanoparticles, ACS Macro Lett., **2019**, 8, 166-171
3. Cui, W.; You, W.; Sun, Z.; Yu, W. Decoupled polymer dynamics in weakly attractive poly(methyl methacrylate)/silica nanocomposites, Macromolecules, **2021**, 54, 5484-5497.
4. Boucher, V.M.; Cangialosi, D.; Alegría, A. J. Colmenero, Enthalpy recovery of PMMA/silica nanocomposites, Macromolecules, **2010**, 43, 7594-7603

5. Priestley, R.D.; Rittigstein, P.; Broadbelt, L.J.; Fukao, K.; Torkelson, J.M. Evidence for the molecular-scale origin of the suppression of physical ageing in confined polymer: fluorescence and dielectric spectroscopy studies of polymer–silica nanocomposites, J. Phys. Condens. Matter, **2007**, 19, Article 205120
6. González-Benito, J.; González-Gaitano, G. Interfacial conformations and molecular structure of PMMA in PMMA/silica nanocomposites. Effect of high-energy ball milling, Macromolecules, **2008**, 41, 4777-4785
7. Lin, Y.; Liu, L.; Xu, G. ; Zhang, D.; Guan, A.; Wu, G. Interfacial interactions and segmental dynamics of poly(vinyl acetate)/silica nanocomposites, J. Phys. Chem. C, 2015, 119, 12956-12966
8. Mingchao, M.; Wenzhi, C.; Yunlong, G.; Wei, Y., Adsorption-desorption effect on physical aging in PMMA-silica nanocomposites, Polymer, **2022**, 255, 125124, https://doi.org/10.1016/j.polymer.2022.125124
9. Rochat, S.; Polak-Kraśna, K.; Tian, M.Timothy J. Mays, Christopher R. Bowen, Andrew D. Burrows, Assessment of the long-term stability of the polymer of intrinsic microporosity PIM-1 for hydrogen storage applications, International Journal of Hydrogen Energy, **2019**, 44(1), 332-337, https://doi.org/10.1016/j.ijhydene.2018.02.175
10. Õige, K.; Avarmaa, T.; Suisalu, A.; Jaaniso, R. Effect of long-term aging on oxygen sensitivity of luminescent Pd-tetraphenylporphyrin/PMMA films, Sensors and Actuators B: Chemical, **2005**, 106(1) ,424-430, https://doi.org/10.1016/j.snb.2004.09.001
11. Gallino, I.; Cangialosi, D.; Evenson, Z.; Schmitt, L.; Hechler, S.; Stolpe, M.; Ruta, B. Hierarchical aging pathways and reversible fragile-to-strong transition upon annealing of a metallic glass former, Acta Materialia, **2018**, 144, 400-410, https://doi.org/10.1016/j.actamat.2017.10.060
12. Vidya, L.; Mandal, B.; Verma, P.K. Review on polymer nanocomposite for ballistic & aerospace applications, Materials Today Proceedings, **2020**, 26, Part 2, 3161-3166, https://doi.org/10.1016/j.matpr.2020.02.652
13. Wypych, A.; Duval, E.; Boiteux, G.; Ulanski, J.; David, L.; Mermet, A. Effect of physical aging on nano- and macroscopic properties of poly(methyl methacrylate) glass, Polymer, **2005**, 46 (26), 12523-12531, https://doi.org/10.1016/j.polymer.2005.10.116
14. Cong-Cong Huang, Chen-Yang Liu, Peculiar α-β relaxations of Syndiotactic-Poly(methyl methacrylate), Polymer, 2021, 225, 2021, 123760, https://doi.org/10.1016/j.polymer.2021.123760
15. Liu, B.; Yu, W. On-demand direct design of polymeric thermal actuator by machine learning algorithm, *Chin. J. Polym. Sci*., **2020**, 38, 908–914.
16. Njuguna, J.; Pielichowski, K. Polymer nanocomposites for aerospace applications: fabrication, Adv. Eng. Mater., **2004**, 6, 193–203.
17. Beiner, M.; Schroter, K.; Hempel, E.; Reissig, S.; E. Donth, E. Multiple glass transition and nanophase separation in poly(n-alkyl methacrylate) homopolymers, Macromolecules, **1999**, 32 (19), 6278–6282.
18. Balasubramanian, K.B.N.; Ramesh, T. Role, effect, and influences of micro and nano-fillers on various properties of polymer matrix composites for microelectronics: a review, Polym. Adv. Technol., **2018**, 29, 1568-1585
19. Cheng, S. et al., Unraveling the mechanism of nanoscale mechanical reinforcement in glassy polymer nanocomposites, Nano Lett., **2016**, 16, 3630–3637
20. Moll, J.; Kumar, S.K. Glass transitions in highly attractive highly filled polymer nanocomposites, Macromolecules, **2012**, 45, 1131–1135.
21. Napolitano, S. Irreversible adsorption of polymer melts and nanoconfinement effects, Soft Matter, **2020**, 16, 5348–5365.
22. Ryan, H. M.; Douglas J. G. Rupert Wimmer, Inverse Gas Chromatography for Determining the Dispersive Surface Free Energy and Acid–Base Interactions of Sheet Molding Compound-Part II Ligno-Cellulosic Fiber Types for Possible Composite Reinforcement, Journal of Applied Polymer Science, **2008**, 110, 3880–3888
23. Gamble, J. F.; Dave, R. N.; Kiang, S.; Leane, M. M.; Tobyn, M.; Wang, S. S.Y. Investigating the applicability of inverse gas chromatography to binary powdered systems: An application of surface heterogeneity profiles to understanding preferential probe-surface interactions, *International Journal of Pharmaceutics*, **2013**, 445, 39– 46
24. Balard, H.; Maafa D.; Santini A.; Donnet J.B. Study by inverse gas chromatography of the surface properties of milled graphites. J. Chromatogr. A, **2008**, 1198–1199, 173–180.
25. Bogillo, V.I.; Shkilev, V.P.; Voelkel, A. Determination of surface free energy components for heterogeneous solids by means of inverse gas chromatography at finite concentrations. J. Mater. Chem., **1998**, 8, 1953–1961.

26. Das, S.C. Zhou, Q.; Morton, D.A.V.; Larson, I.; Stewart, P.J. Use of surface energy distributions by I;nverse gas chromatography to understand mechanofusion processing and functionality of lactose coated with magnesium stearate. Eur. J. Pharm. Sci., **2011**, 43, 325–333.
27. Das, S.C.; Stewart, P.J. Characterising surface energy of pharmaceutical powders by inverse gas chromatography at finite dilution. J. Pharm. Pharmacol. **2012**, 64, 1337–1348.
28. Stella K. Papadopoulou, Costas Panayiotou, Assessment of the thermodynamic properties of poly(2,2,2-trifluoroethyl methacrylate) by inverse gas chromatography, Journal of Chromatography A, 1324 (2014) 207– 214. https://doi.org/10.1016/j.chroma.2013.11.044.
29. Saint-Flour, C.; Papirer, E.; Gas-solid chromatography. A method of measuring surface free energy characteristics of short carbon fibers. 1. Through adsorption isotherms, *Ind. Eng. Chem. Prod. Res. Dev.*, **1982**, 21, 337-341, https://doi.org/10.1021/i300006a029.
30. Saint-Flour, C.; Papirer, E.; Gas-solid chromatography: method of measuring surface free energy characteristics of short fibers. 2. Through retention volumes measured near zero surface coverage, *Ind. Eng. Chem. Prod. Res. Dev.*, **1982**, 21, 666-669, https://doi.org/10.1021/i300008a031.
31. Saint-Flour, C.; Papirer, E.; Gas-solid chromatography: a quick method of estimating surface free energy variations induced by the treatment of short glass fibers. *J. Colloid Interface Sci.* ***1983***, 91, 69-75. https://doi.org/10.1016/0021-9797(83)90314-4
32. Schultz, J.; Lavielle, L.; Martin, C. The role of the interface in carbon fibre-epoxy composites. *J. Adhes.*, **1987**, 23, 45–60, https://doi.org/10.1080/00218468708080469.
33. Donnet, J.-B.; Park, S.; Balard, H. Evaluation of specific interactions of solid surfaces by inverse gas chromatography, *Chromatographia*, **1991**, 31, 434–440. https://doi.org/10.1007/BF02262385
34. Brendlé, E.; Papirer, E. A new topological index for molecular probes used in inverse gas chromatography for the surface nanorugosity evaluation, 2. Application for the Evaluation of the Solid Surface Specific Interaction Potential, *J. Colloid Interface Sci.*, **1997**, 194, 217–2224. https://doi.org/10.1006/jcis.1997.5105
35. Brendlé, E.; Papirer, E. A new topological index for molecular probes used in inverse gas chromatography for the surface nanorugosity evaluation, 1. Method of Evaluation, *J. Colloid Interface Sci.* **1997**, 194, 207–216. https://doi.org/10.1006/jcis.1997.5105
36. Sawyer, D.T.; Brookman. D.J. Thermodynamically based gas chromatographic retention index for organic molecules using salt-modified aluminas and porous silica beads, *Anal. Chem*. **1968**, 40, 1847-1850. https://doi.org/10.1021/ac60268a015.
37. Chehimi, M.M.; Pigois-Landureau, E. Determination of acid–base properties of solid materials by inverse gas chromatography at infinite dilution. A novel empirical method based on the dispersive contribution to the heat of vaporization of probes, *J. Mater. Chem.*, **1994**, 4, 741–745. https://doi.org/10.1039/JM9940400741
38. Hamieh, T. New methodology to study the dispersive component of the surface energy and acid–base properties of silica particles by inverse gas chromatography at infinite dilution, *Journal of Chromatographic Science*, **2022**, 60 (2), 126-142, https://doi.org/10.1093/chromsci/bmab066
39. Hamieh, T.; Schultz, J. New approach to characterize physicochemical properties of solid substrates by inverse gas chromatography at infinite dilution. Some new methods to determine the surface areas of some molecules adsorbed on solid surfaces. *J. Chromatogr. A*, **2002**, *969*, 17–47. https://doi.org/10.1016/S0021-9673(02)00368-0.
40. Voelkel, A. Inverse gas chromatography: characterization of polymers, fibers, modified silicas, and surfactants. *Crit Rev Anal Chem.* **1991**, 22, 411-439. https://doi.org/10.1080/10408349108051641.
41. Hamieh, T.; Ahmad, A.A.; Roques-Carmes, T.; Toufaily, J. New approach to determine the surface and interface thermodynamic properties of H-β-zeolite/rhodium catalysts by inverse gas chromatography at infinite dilution. *Sci. Rep.* **2020**, *10*, 20894. https://doi.org/10.1038/s41598-020-78071-1.
42. Hamieh, T. New Methodology to Study the Dispersive Component of the Surface Energy and Acid–Base Properties of Silica Particles by Inverse Gas Chromatography at Infinite Dilution. *J. Chromatogr. Sci.* **2021**, *60*, 126–142. https://doi.org/10.1093/chromsci/bmab066.
43. Hamieh, T. New physicochemical methodology for the determination of the surface thermodynamic properties of solid particles. *Appliedchem*, **2023**, *3*, 229–255. https://doi.org/10.3390/appliedchem3020015.
44. Hamieh, T. New Progress on London Dispersive Energy, Polar Surface Interactions, and Lewis's Acid–Base Properties of Solid Surfaces, Molecules, **2024**, 29 (5), 949, https://doi.org/10.3390/molecules29050949

45. Hamieh, T. London Dispersive and Lewis Acid-Base Surface Energy of 2D Single-Crystalline and Polycrystalline Covalent Organic Frameworks, *Crystals,* **2024**, *14*(2), 148; https://doi.org/10.3390/cryst14020148
46. Hamieh, T. Inverse Gas Chromatography to Characterize the Surface Properties of Solid Materials, *Chem. Mater.* 2024, 2024, https://doi.org/10.1021/acs.chemmater.3c03091
47. A. Voelkel, B. Strzemiecka, K. Adamska, K. Milczewska, Inverse gas chromatography as a source of physiochemical data, J. Chromatogr. A, **2009**, 1216, 1551. https://doi.org/10.1016/j.chroma.2008.10.096
48. G.S. Dritsas, K. Karatasos, C. Panayiotou, Investigation of thermodynamic properties of hyperbranched aliphatic polyesters by inverse gas chromatography, J. Chromatogr. A, **2009**, 1216 (51), 8979-8985, https://doi.org/10.1016/j.chroma.2009.10.050.
49. S.K. Papadopoulou, C. Panayiotou, Thermodynamic characterization of poly(1,1,1,3,3,3-hexafluoroisopropyl methacrylate) by inverse gas chromatography**,** J. Chromatogr. A, **2012**, 1229 (2012) 230-236. https://doi.org/10.1016/j.chroma.2012.01.055
50. J.F. Gamble, R.N. Dave, S. Kiang, M.M. Leane, M. Tobyn, S.S.Y. Wang, Investigating the applicability of inverse gas chromatography to binary powdered systems: An application of surface heterogeneity profiles to understanding preferential probe-surface interactions, Int. J. Pharm., **2013**, 445, 39-46. https://doi.org/10.1016/j.ijpharm.2013.01.061
51. J. Kołodziejek, A. Voelkel, K. Heberger, Characterization of hybrid materials by means of inverse gas chromatography and chemometrics, J. Pharm. Sci., **2013**, 102, 15241531. https://doi.org/10.1002/jps.23489
52. Lazar, Petr, František Karlický, Petr Jurečka, M. Kempka V. Kocman, Eva Otyepková, Klára Šafářová and Michal Otyepka. "Adsorption of small organic molecules on graphene." *Journal of the American Chemical Society*, ***2013***, 135 (16), 6372-6372. https://doi.org/10.1021/ja403162r
53. M.N. Belgacem, G. Czeremuszkin, S. Sapieha, A. Gandini, Surface by XPS characterization and inverse gas of cellulose fibres chromatography, Cellulose, **1995**, 2, 145157, https://doi.org/10.1007/BF00813015
54. Papadopoulou, Stella K., Costas Tsioptsias, Alex K. Pavlou, Kyriakos Kaderides, Steven Sotiriou and Costas Panayiotou. "Superhydrophobic surfaces from hydrophobic or hydrophilic polymers via nanophase separation or electrospinning/electrospraying. *Colloids and Surfaces A: Physicochemical and Engineering Aspects,* ***2011***, 387, 71-78. https://doi.org/10.1016/J.COLSURFA.2011.07.028
55. Hamieh T., Rezzaki M., Schultz J., Study of the second order transitions and acid-base properties of polymers adsorbed on oxides, by using inverse gas chromatography at infinite dilution, I and II, *J. Colloid Interface Sci.*, **2001**, 233 (2), 339-347. https://doi.org/10.1006/jcis.2000.7267.
56. Hamieh, T. Study of the Specific Entropy of Poly (α-n-alkyl) Methacrylates Adsorbed on Alumina or Silica by Inverse Gas Chromatography (IGC), **2011**, *Soft Materials*, 9 (1), 15 – 31. https://doi.org/10.1080/1539445X.2010.521608
57. Hamieh, T. New Approach for the Determination of Acid Base Properties of Poly(α-n-alkyl) Methacrylates Adsorbed on Silica by Inverse Gas Chromatography (IGC), *Chromatographia,* **2011**, 73 (7-8), 709-719. https://doi.org/10.1007/S10337-011-1925-6
58. Hamieh, T.; Toufaily, J.; Mouneimné, A.B. Effect of the Tacticity of PMMA Adsorbed on Alumina and Silica on the Specific Entropy Change of Polymer by Inverse GC, Chromatographia, **2011**, 73 (1-2), 99-107. https://doi.org/10.1007/S10337-010-1824-2
59. Papirer E.; Perrin J.-M.; Siffert B.; Philipponneau G. Surface characteristics of aluminas in relation with polymer adsorption, J. Colloid Interface Sci., **1991**, 144, 263–270, https://doi.org/10.1016/0021-9797(91)90257-9
60. Gutmann, V. The Donor-acceptor Approach to Molecular Interactions, Plenum. New York, 1978.
61. Riddle, F. L.; Fowkes, F. M. Spectral shifts in acid-base chemistry. Van der Waals contributions to acceptor numbers, Spectral shifts in acid-base chemistry. 1. van der Waals contributions to acceptor numbers. *J. Am. Chem. Soc.*, **1990**, 112 (9), 3259-3264. https://doi.org/10.1021/ja00165a001.

 doi:10.20944/preprints202403.0997.v1

62. Hamieh, T.; Rezzaki M.; Schultz, J. Study of the transition temperatures and acid-base properties of poly (methyl methacrylate) adsorbed on alumina and silica, by using inverse gas chromatography technique, *Colloids and Surfaces A: Physicochemical and Engineering Aspects*, **2001**, 189 (1-3), 279-291. https://doi.org/10.1016/S0927-7757(01)00597-0
63. David R. Lide, ed., *CRC Handbook of Chemistry and Physics, Internet Version 2007, (87th Edition), <http:/www.hbcpnetbase.com>*, Taylor and Francis, Boca Raton, FL, 2007.